

Advanced School on  
**QUANTUM MODELLING**  
of Materials with CRYSTAL

## **Strain-Related Tensorial Properties of Solids: Elasticity, Photo-Elasticity, Piezoelectricity, Piezo-Optics**

*QMMC2026, January 2026, Volta Redonda – Rio de Janeiro, Brazil*

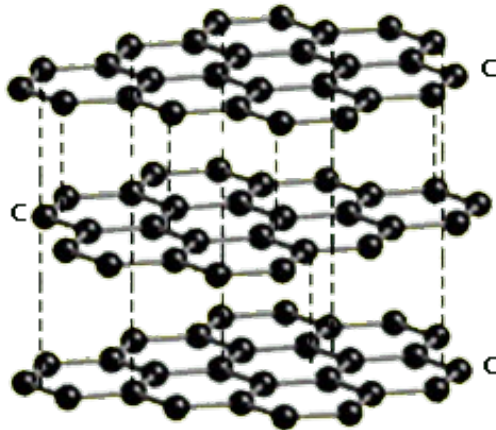
Alessandro Erba

Dipartimento di Chimica, Università di Torino (Italy)  
[alessandro.erba@unito.it](mailto:alessandro.erba@unito.it)

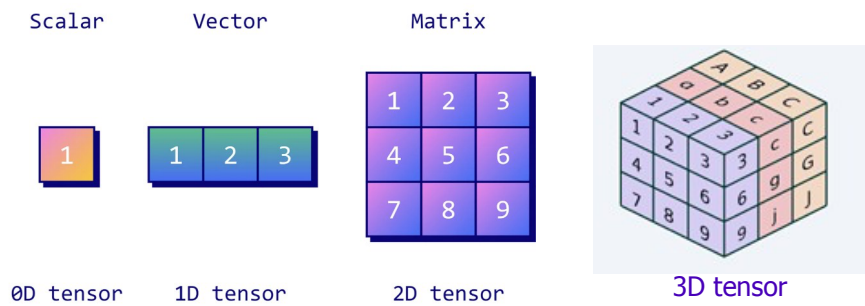


# Lattice Anisotropy and Physical Tensors

Because of their **anisotropic structure**, many **physical properties of crystals** require a **tensorial representation** (often Cartesian).



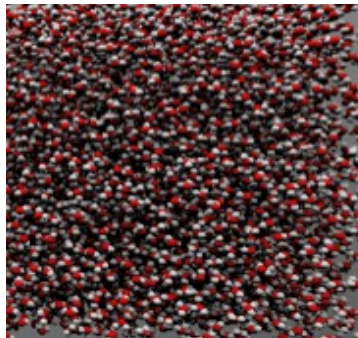
The same physical property may take different values “along” different crystallographic directions.





# Lattice Anisotropy and Physical Tensors

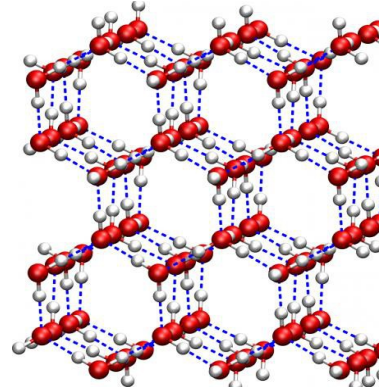
For instance, the **dielectric response**:



Liquid water

For a liquid

Dielectric constant  $\epsilon$



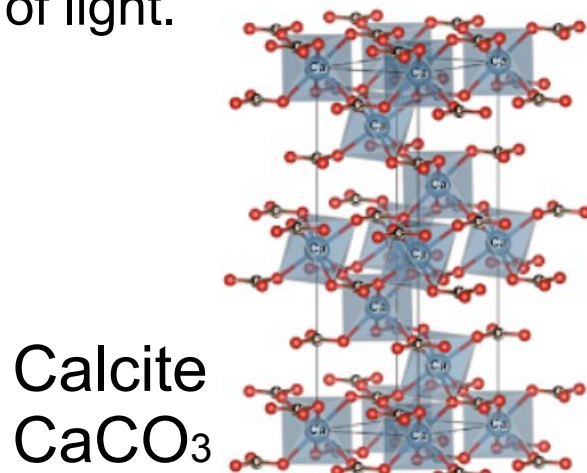
Ice

For a crystal

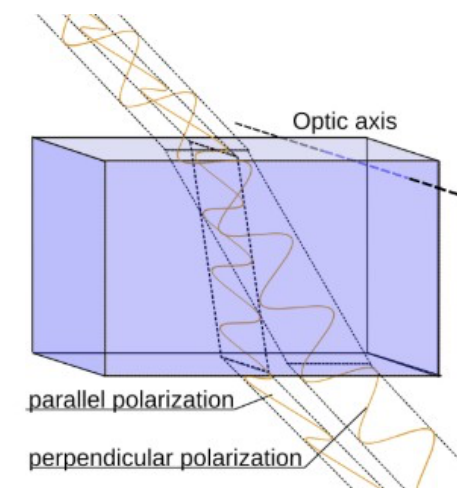
Dielectric tensor  $\boldsymbol{\epsilon}$

$$\boldsymbol{\epsilon} = \epsilon_0 \begin{bmatrix} \epsilon_{11} & \epsilon_{12} & \epsilon_{13} \\ \epsilon_{21} & \epsilon_{22} & \epsilon_{23} \\ \epsilon_{31} & \epsilon_{32} & \epsilon_{33} \end{bmatrix}$$

Birefringence, also called double refraction, is the optical property of a material having a refractive index that depends on the polarization and propagation direction of light.



Calcite  
 $\text{CaCO}_3$





# Lattice Anisotropy and Physical Tensors

A variety of **physical properties** can be defined in terms of **energy derivatives** wrt different types of “**perturbations**”:

- Electric field(s)
  - Magnetic field(s)
  - Atomic displacement(s)
  - Lattice distortion(s)
  - Temperature
  - ...
- } Cartesian vectors (i.e. first-rank tensors)

A **rigorous formal description** of the properties that can be obtained as (**mixed**) **energy derivatives up to second-order** can be found in:

X. Wu, D. Vanderbilt and D.R. Hamann, *Phys. Rev. B*, **72**, 035105 (2005)

And **up to third-order** in:

M. Veithen, X. Gonze and P. Ghosez, *Phys. Rev. B*, **71**, 125107 (2005)



# Lattice Anisotropy and Physical Tensors

## Molecular Systems



$$\text{property} \propto \left( \frac{d}{dF} \right)^f \left( \frac{d}{dB} \right)^b \left( \frac{d}{dI} \right)^i \left( \frac{d}{dR} \right)^r E \Big|_0$$

$f$	$b$	$i$	$r$	property
-----	-----	-----	-----	----------

1	0	0	0	Dipole moment
2	0	0	0	Polarizability
3	0	0	0	First-Hyperpolarizability
4	0	0	0	Second-Hyperpolarizability

...

0	0	0	1	Atomic forces
0	0	0	2	Harmonic interatomic force constants
0	0	0	3	Anharmonic (cubic) interatomic force constants

...



# Lattice Anisotropy and Physical Tensors

## Molecular Systems

	Electric Field	Magnetic Field	Nuclear Spin	Atomic Positions
--	-------------------	-------------------	-----------------	---------------------

$$\text{property} \propto \left( \frac{d}{dF} \right)^f \left( \frac{d}{dB} \right)^b \left( \frac{d}{dI} \right)^i \left( \frac{d}{dR} \right)^r E \Big|_0$$

f	b	i	r	property
1	1	0	0	circular dichroism
1	0	0	1	infra-red absorption intensities
0	1	1	0	nuclear magnetic shielding
2	1	0	0	magnetic circular dichroism (Faraday effect)
2	0	0	1	Raman intensities
1	0	0	2	infra-red intensities for overtone and hot bands
2	2	0	0	Cotton–Mouton effect
2	0	0	2	Raman intensities for overtone and hot bands
...	...			
...	...			



# Lattice Anisotropy and Physical Tensors

## Periodic Systems



$$\text{property} \propto \left( \frac{d}{dF} \right)^f \left( \frac{d}{dB} \right)^b \left( \frac{d}{dI} \right)^i \left( \frac{d}{dR} \right)^r \left( \frac{d}{dA} \right)^a E \Big|_0$$

f	b	i	r	a	property
---	---	---	---	---	----------

0 0 0 0 1 Stress tensor

0 0 0 0 2 Elastic constants

0 0 0 0 3 Third-order elastic constants (TOECs)

...

0 0 0 1 1 Internal strain constants

...

1 0 0 0 1 Piezoelectric constants

0 1 0 0 1 Magneto-elastic coupling constants

...

2 0 0 0 1 Photo-elastic and Piezo-optic constants



# Lattice Anisotropy and Physical Tensors

## Periodic Systems



$$\text{property} \propto \left( \frac{d}{dF} \right)^f \left( \frac{d}{dB} \right)^b \left( \frac{d}{dI} \right)^i \left( \frac{d}{dR} \right)^r \left( \frac{d}{dA} \right)^a E \Big|_0$$

f	b	i	r	a	property
---	---	---	---	---	----------

0 0 0 0 1 **Stress tensor**

0 0 0 0 2 **Elastic constants**

0 0 0 0 3 Third-order elastic constants (TOECs)

...

0 0 0 1 1 **Internal strain constants**

...

1 0 0 0 1 **Piezoelectric constants**

0 1 0 0 1 Magneto-elastic coupling constants

...

2 0 0 0 1 **Photo-elastic and Piezo-optic constants**



# Lattice Anisotropy and Physical Tensors

## Periodic Systems



$$\text{property} \propto \left( \frac{d}{dF} \right)^f \left( \frac{d}{dB} \right)^b \left( \frac{d}{dI} \right)^i \left( \frac{d}{dR} \right)^r \left( \frac{d}{dA} \right)^a E \Big|_0$$

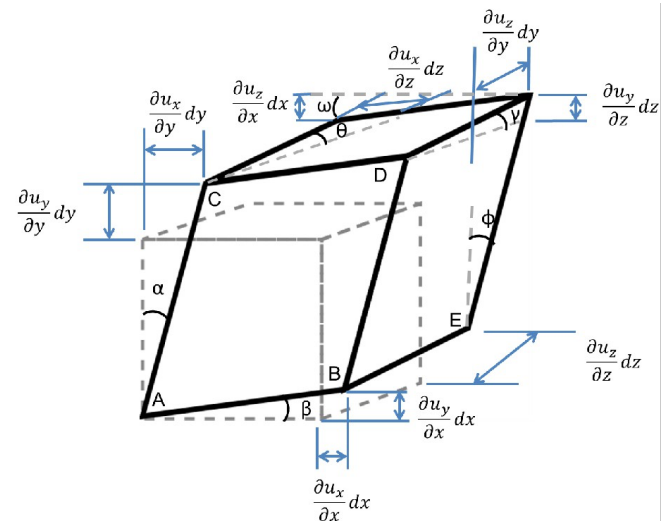
f	b	i	r	a	property	Order	Rank
0	0	0	0	1	<b>Stress tensor</b>	1	2
0	0	0	0	2	<b>Elastic constants</b>	2	4
0	0	0	0	3	Third-order elastic constants (TOECs)		
...							
0	0	0	1	1	<b>Internal strain constants</b>	2	3
...							
1	0	0	0	1	<b>Piezoelectric constants</b>	2	3
0	1	0	0	1	Magneto-elastic coupling constants		
...							
2	0	0	0	1	<b>Photo-elastic and Piezo-optic constants</b>	3	4



# Stress and Strain

The **strain** of a given 3D lattice configuration relative to an unstrained reference is measured by the second-rank strain tensor  $\epsilon$  (sometimes  $\eta$ ):

$$\begin{bmatrix} \varepsilon_{11} & \varepsilon_{12} & \varepsilon_{13} \\ \varepsilon_{21} & \varepsilon_{22} & \varepsilon_{23} \\ \varepsilon_{31} & \varepsilon_{32} & \varepsilon_{33} \end{bmatrix} = \begin{bmatrix} \frac{1}{2}\left(\frac{\partial u_1}{\partial x_1} + \frac{\partial u_1}{\partial x_1}\right) & \frac{1}{2}\left(\frac{\partial u_1}{\partial x_2} + \frac{\partial u_2}{\partial x_1}\right) & \frac{1}{2}\left(\frac{\partial u_1}{\partial x_3} + \frac{\partial u_3}{\partial x_1}\right) \\ \frac{1}{2}\left(\frac{\partial u_2}{\partial x_1} + \frac{\partial u_1}{\partial x_2}\right) & \frac{1}{2}\left(\frac{\partial u_2}{\partial x_2} + \frac{\partial u_2}{\partial x_2}\right) & \frac{1}{2}\left(\frac{\partial u_2}{\partial x_3} + \frac{\partial u_3}{\partial x_2}\right) \\ \frac{1}{2}\left(\frac{\partial u_3}{\partial x_1} + \frac{\partial u_1}{\partial x_3}\right) & \frac{1}{2}\left(\frac{\partial u_3}{\partial x_2} + \frac{\partial u_2}{\partial x_3}\right) & \frac{1}{2}\left(\frac{\partial u_3}{\partial x_3} + \frac{\partial u_3}{\partial x_3}\right) \end{bmatrix}$$



The **anti-symmetric** part of this tensor corresponds to a **pure rotation**. We are interested in the **symmetric** part of the tensor corresponding to a **pure strain**. Under a pure strain, lattice parameters are transformed as follows:

$$a'_{\alpha j} = \sum_k (\delta_{jk} + \epsilon_{jk}) a_{\alpha k} \quad \text{with}$$

$$\begin{pmatrix} \vec{a}_1 \\ \vec{a}_2 \\ \vec{a}_3 \end{pmatrix} = \begin{pmatrix} a_{1x} & a_{1y} & a_{1z} \\ a_{2x} & a_{2y} & a_{2z} \\ a_{3x} & a_{3y} & a_{3z} \end{pmatrix} = \begin{pmatrix} a_{11} & a_{12} & a_{13} \\ a_{21} & a_{22} & a_{23} \\ a_{31} & a_{32} & a_{33} \end{pmatrix}$$



# Stress and Strain

The pure strain tensor is symmetric and thus there are only 6 independent components:

$$\epsilon = \begin{bmatrix} \epsilon_{11} & \epsilon_{12} & \epsilon_{13} \\ \epsilon_{21} & \epsilon_{22} & \epsilon_{23} \\ \epsilon_{31} & \epsilon_{32} & \epsilon_{33} \end{bmatrix}$$

A more compact **one-index (Voigt) notation** is often adopted for the strain tensor, with Voigt's indices  $v, u = 1, \dots, 6$

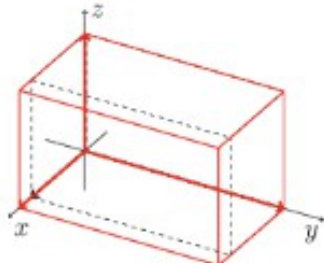
$$\epsilon = \begin{bmatrix} \epsilon_1 \\ \epsilon_2 \\ \epsilon_3 \\ \epsilon_4 \\ \epsilon_5 \\ \epsilon_6 \end{bmatrix} \quad \begin{array}{l} 1 = xx \\ 2 = yy \\ 3 = zz \\ 4 = yz \\ 5 = xz \\ 6 = xy \end{array}$$



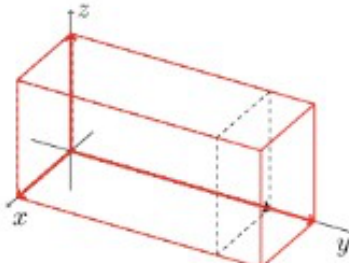
# Stress and Strain

The 6 fundamental strain components are the following:

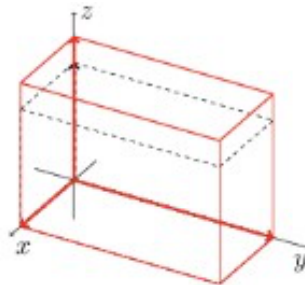
## Normal



$$\varepsilon_1 = \varepsilon_{xx}$$

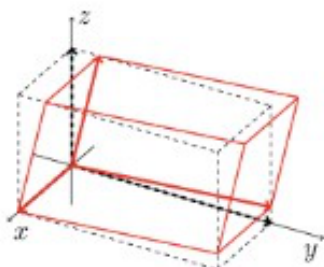


$$\varepsilon_2 = \varepsilon_{yy}$$

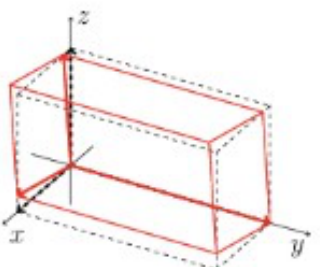


$$\varepsilon_3 = \varepsilon_{zz}$$

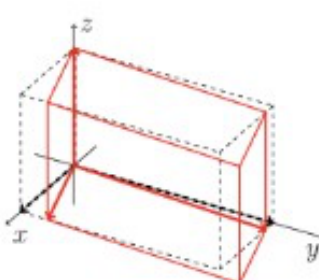
## Shear



$$\varepsilon_4 = \varepsilon_{yz}$$



$$\varepsilon_5 = \varepsilon_{xz}$$



$$\varepsilon_6 = \varepsilon_{xy}$$



# Stress and Strain

In CRYSTAL, first-order derivatives of the energy with respect to lattice parameter distortions (**cell forces**) are computed **analytically**.

$$\frac{\partial E}{\partial a_{\alpha i}}$$

where  $\alpha = 1, \dots, P$  (with  $P = 1, 2, 3$  being the periodicity of the lattice), and  $i = x, y, z$  being a Cartesian index.

K. Doll, R. Dovesi and R. Orlando, Theor. Chem. Acc. 112, 394 (2004) for 3D

K. Doll, R. Dovesi and R. Orlando, Theor. Chem. Acc. 115, 354 (2006) for 1D and 2D

First-derivatives of the energy with respect to strain components can be obtained from quantities above simply as:

$$\frac{\partial E}{\partial \epsilon_{ij}} = \sum_{\alpha} \frac{\partial E}{\partial a_{\alpha i}} a_{\alpha j}$$

which (almost) constitute the elements of the **stress tensor  $\sigma$** .



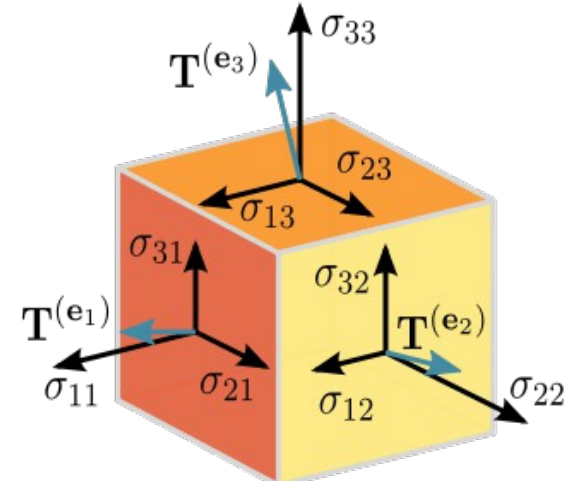
# Stress and Strain

The elements of the **stress tensor** are indeed defined as:

$$\sigma_{ij} = \frac{1}{V} \frac{\partial E}{\partial \epsilon_{ij}}$$

Clearly, it is in turn a symmetric second-rank tensor:

$$\begin{pmatrix} \sigma_{11} & \sigma_{12} & \sigma_{13} \\ \sigma_{12} & \sigma_{22} & \sigma_{23} \\ \sigma_{13} & \sigma_{23} & \sigma_{33} \end{pmatrix} = \begin{pmatrix} \sigma_1 & \sigma_6 & \sigma_5 \\ \sigma_6 & \sigma_2 & \sigma_4 \\ \sigma_5 & \sigma_4 & \sigma_3 \end{pmatrix}$$



In CRYSTAL, it was implemented by Klaus Doll back in 2010.

K. Doll, Mol. Phys., 108(3–4), 223–227 (2010)

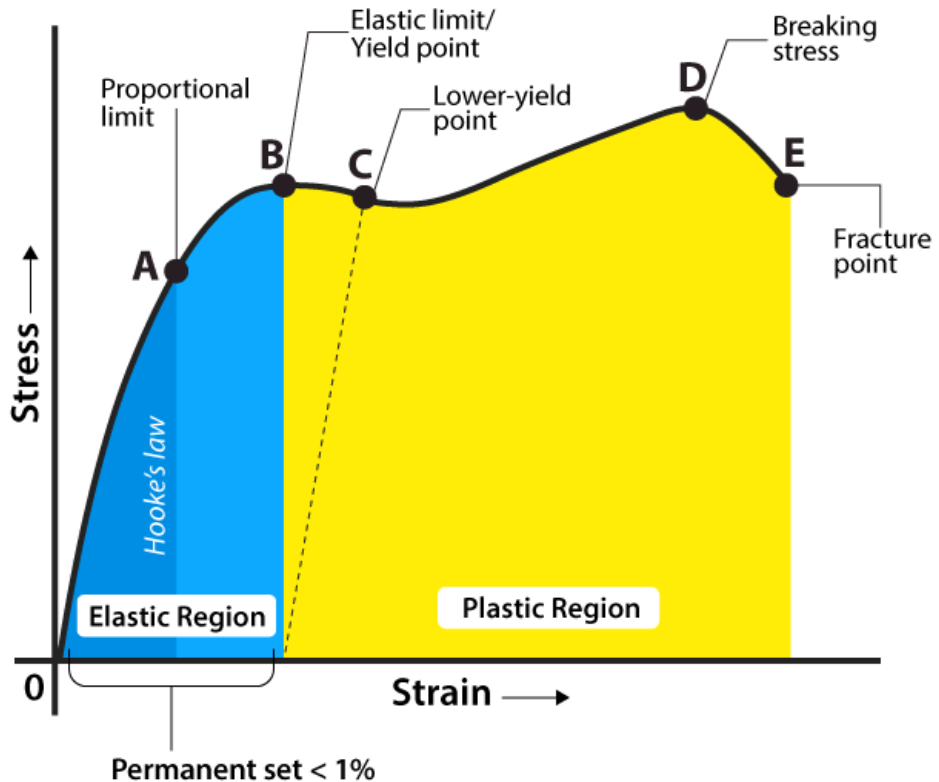
Let us note that, in the case of a **hydrostatic pressure  $p$** , the stress tensor takes the form:

$$\sigma_{ij} = -p\delta_{ij}$$



# Stress and Strain

The **stress-strain relationship** describes how a material deforms (strain) under an applied force (stress), revealing properties like elasticity, yield strength, and ductility through a stress-strain curve:

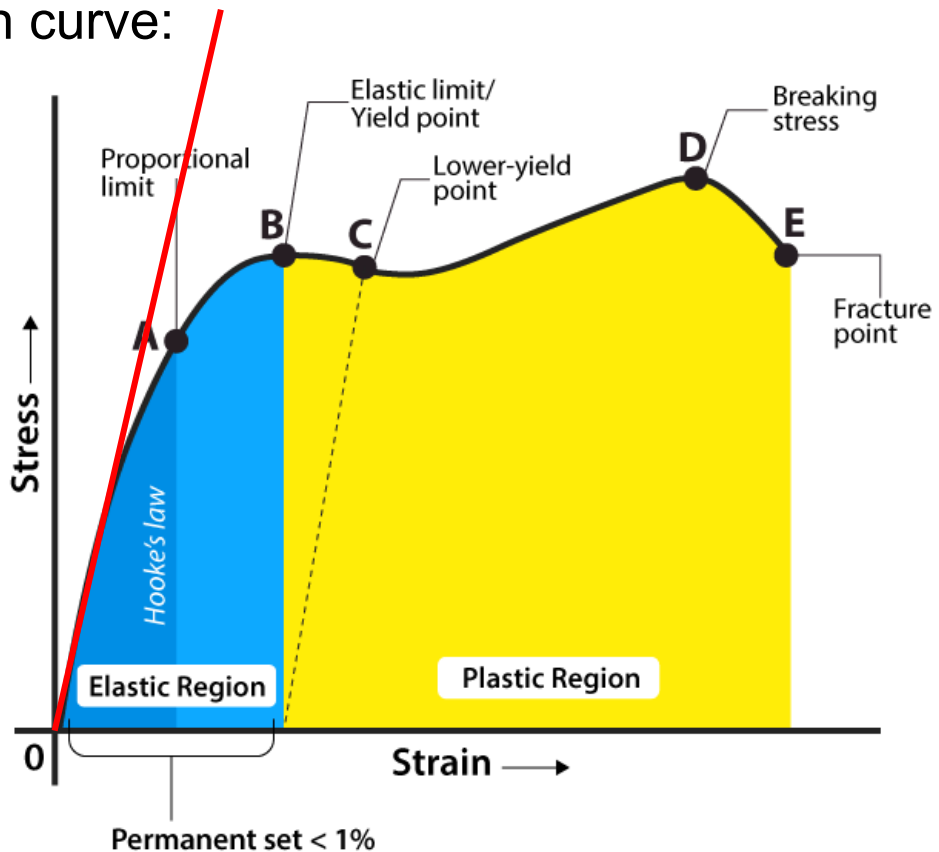


The **stress is proportional to strain in the elastic region** (**Hooke's law**) and the **slope is Young's modulus** but becomes non-linear as the material yields or fractures. The end of this stage is the initiation point of **plastic deformation**.



# Stress and Strain

The **stress-strain relationship** describes how a material deforms (strain) under an applied force (stress), revealing properties like elasticity, yield strength, and ductility through a stress-strain curve:

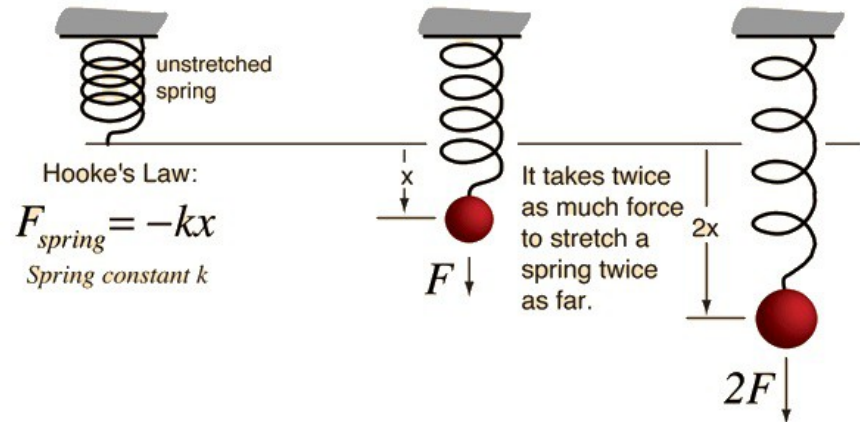


The **stress is proportional to strain in the elastic region (Hooke's law)** and the **slope is Young's modulus** but becomes non-linear as the material yields or fractures. The end of this stage is the initiation point of **plastic deformation**.



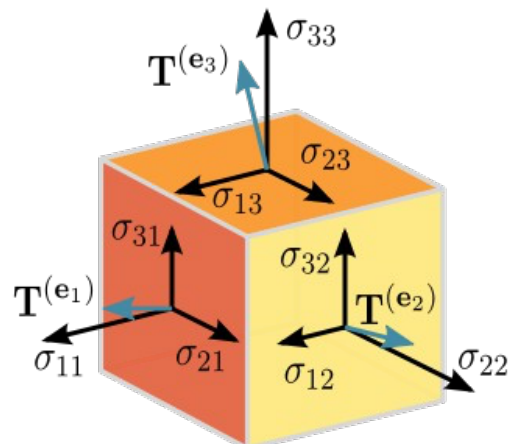
# Stress and Strain

Hooke's law (**elasticity**) in 1D where stress and strain are both uniaxial and can thus be represented by two scalar quantities:



$$\sigma = k\epsilon \quad k = \frac{\partial \sigma}{\partial \epsilon}$$

Generalized Hooke's law (**elasticity**) for a 3D anisotropic medium where both stress and strain are second-rank tensors:



$$\sigma_{ij} = \sum_{kl} C_{ijkl} \epsilon_{kl}$$

$$C_{ijkl} = \frac{\partial \sigma_{ij}}{\partial \epsilon_{kl}} = \frac{1}{V} \frac{\partial^2 E}{\partial \epsilon_{ij} \partial \epsilon_{kl}}$$



# Elastic Tensor

They are the so-called elastic stiffness constants and represent the elements of a **fourth-rank elastic tensor  $C$** :

$$C_{ijkl} = \frac{1}{V} \frac{\partial^2 E}{\partial \epsilon_{ij} \partial \epsilon_{kl}}$$

with  $3 \times 3 \times 3 \times 3 = 81$  elements (!). The elastic tensor **fully describes the mechanical elastic response of a material**. As the strain tensor is symmetric and has only six independent components, the description can be simplified resorting to Voigt's notation:

$$C_{vu} = \frac{1}{V} \frac{\partial^2 E}{\partial \epsilon_v \partial \epsilon_u}$$

According to which the elastic tensor becomes a  $6 \times 6$  matrix with **36** elements. Inspection of the equation above reveals that this matrix is symmetric:

$$C_{vu} = C_{uv}$$

which further reduces the number of independent constants to **21**.

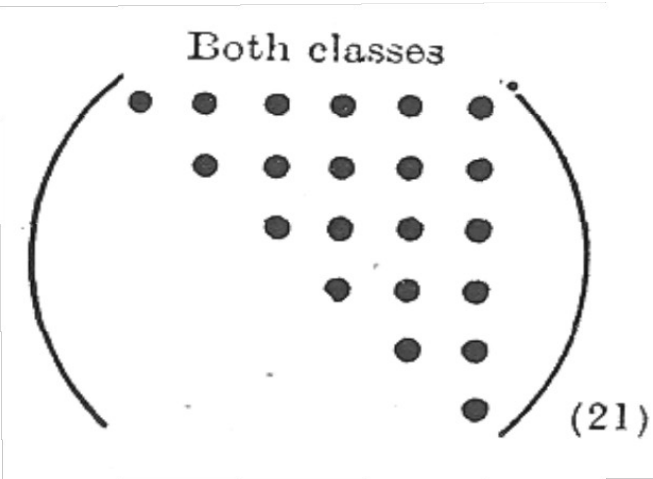
# Elastic Tensor



The picture can be further simplified by **Neumann's Principle** (or symmetry principle) that states that the symmetry of a material's physical property (like electrical, optical, elastic, etc.) must include all the symmetry elements of the crystal's point group; the properties can have higher symmetry but never lower symmetry than the underlying crystal structure, effectively setting a lower limit on property symmetry and guiding material design.

$$C_{vu} = \frac{1}{V} \frac{\partial^2 E}{\partial \epsilon_v \partial \epsilon_u}$$

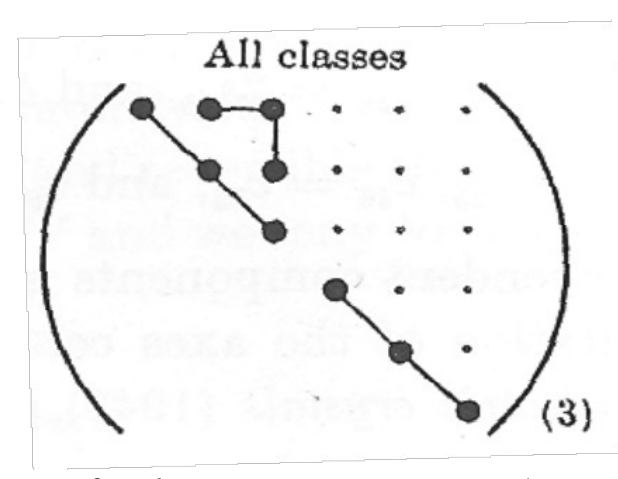
Triclinic



Hexagonal



Cubic



J. F. Nye, *Oxford University Press*, (1985)



# Elastic Tensor – Clamped Nuclei Term

Strain-induced tensorial properties of solids can be formally decomposed into a purely **electronic “clamped-nuclei”** term due to the **instantaneous electronic response to strain**, and into a **nuclear-relaxation** term due to the rearrangement of atomic positions upon strain.

$$C_{vu} = \frac{1}{V} \frac{\partial^2 E}{\partial \epsilon_v \partial \epsilon_u} = C_{vu}^{\text{ele}} + C_{vu}^{\text{nuc}}$$

$$C_{vu}^{\text{ele}} = \frac{1}{V} \left. \frac{\partial^2 E}{\partial \epsilon_v \partial \epsilon_u} \right|_{\text{at. displ.}}$$

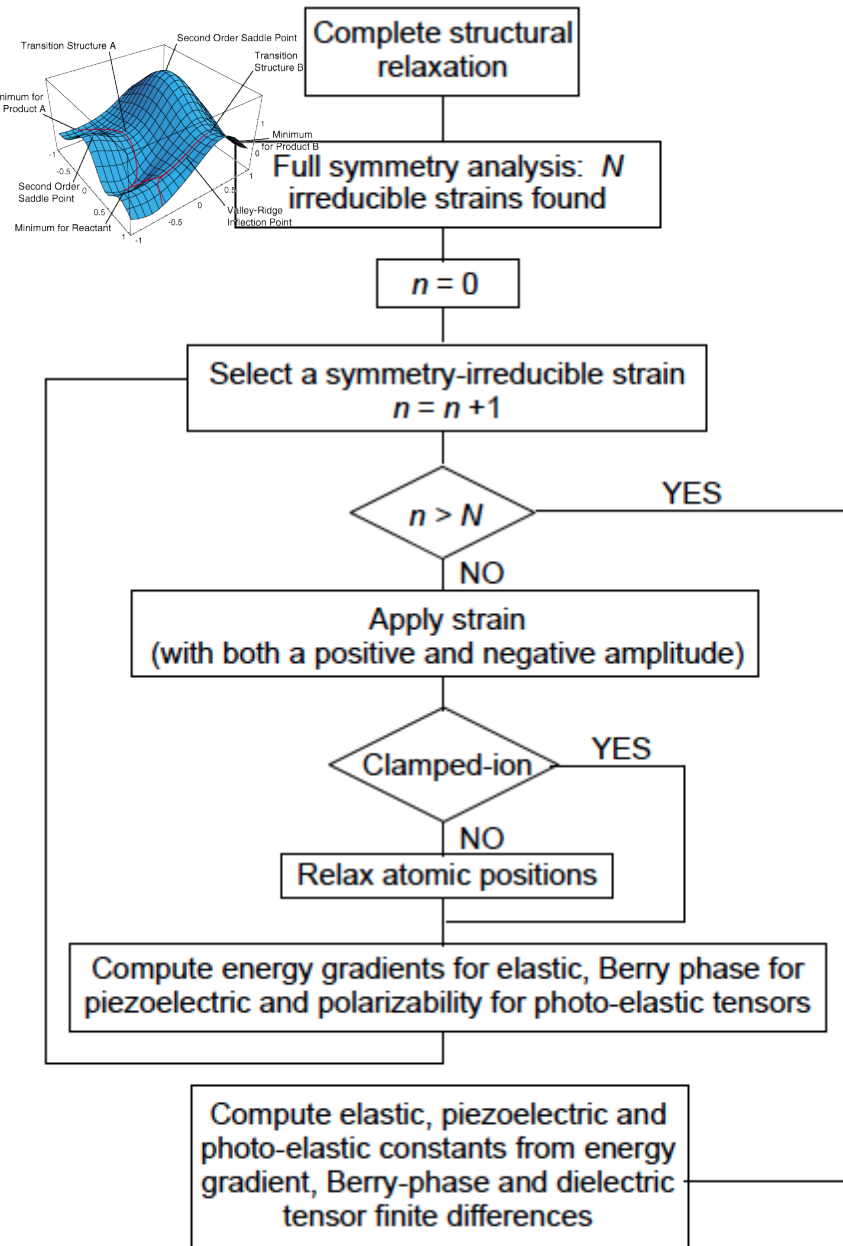
In CRYSTAL, the second energy derivatives of the electronic clamped-nuclei term are computed from finite differences of analytical forces:

$$C_{vu}^{\text{ele}} = \frac{1}{V} \left. \frac{\partial^2 E}{\partial \epsilon_v \partial \epsilon_u} \right|_{\text{at. displ.}} = \frac{1}{V} \left. \frac{\partial f_v}{\partial \epsilon_u} \right|_{\text{at. displ.}} \quad \text{with} \quad f_v = \frac{\partial E}{\partial \epsilon_v}$$

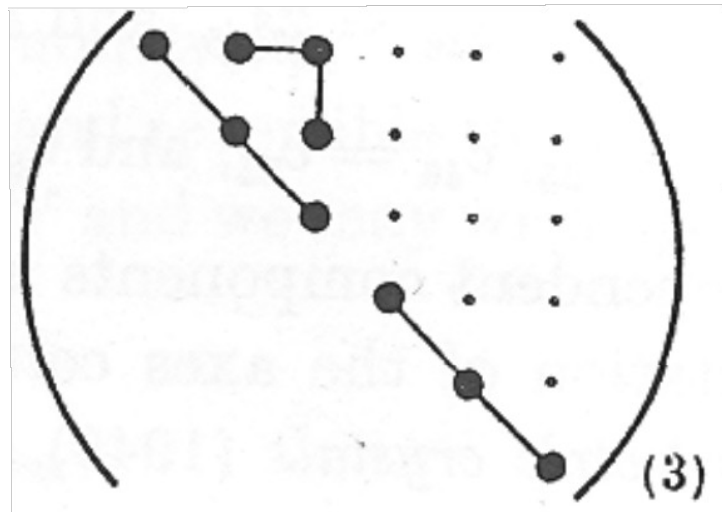
$$C_{vu}^{\text{ele}} = \frac{1}{V} \frac{f_v|_{\epsilon_u=+\delta} - f_v|_{\epsilon_u=-\delta}}{2\delta}$$



# Elastic Tensor – Clamped Nuclei Term



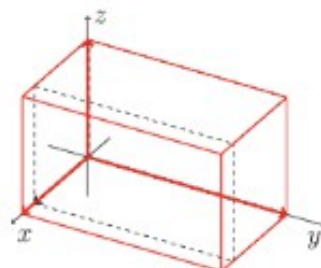
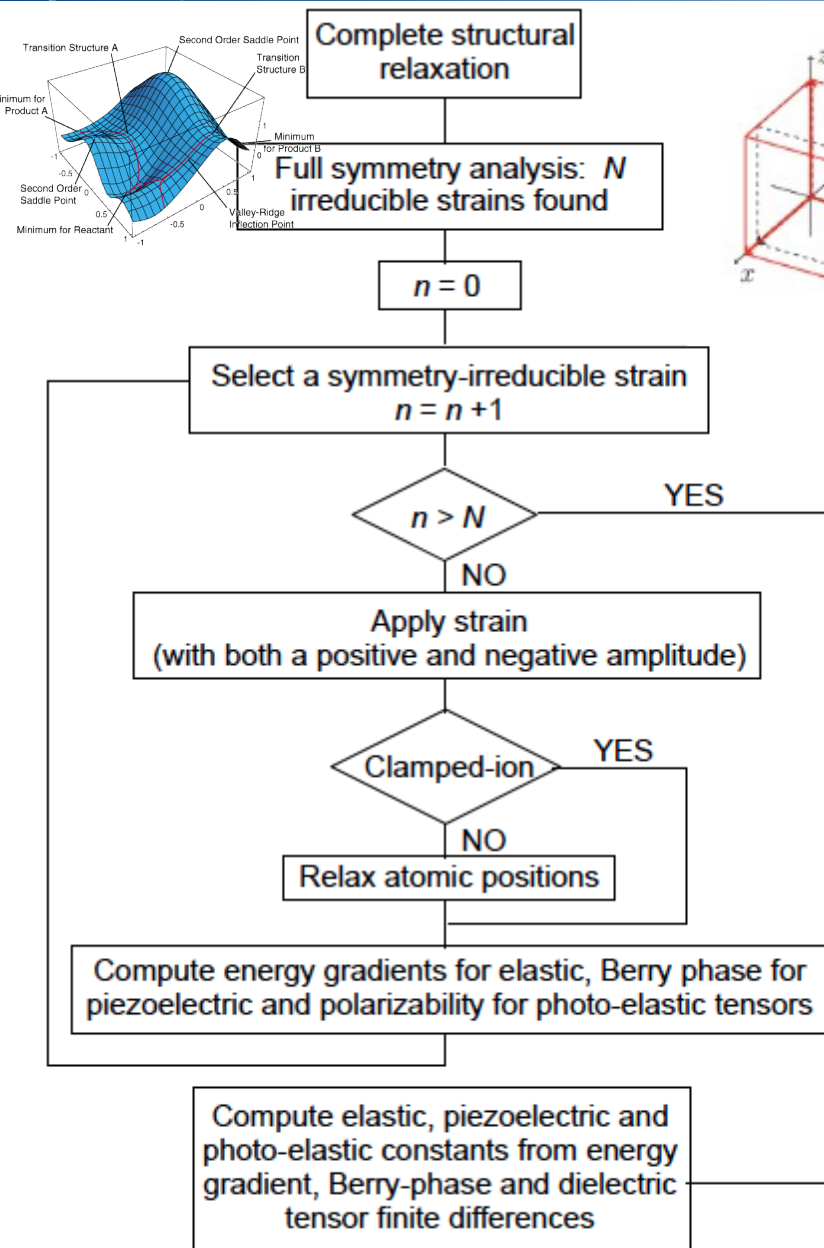
$$C_{vu}^{\text{ele}} = \frac{1}{V} \frac{f_v|_{\epsilon_u=+\delta} - f_v|_{\epsilon_u=-\delta}}{2\delta}$$



For a cubic lattice for instance, there are only 2 symmetry-independent strains:  $\epsilon_1$  and  $\epsilon_4$

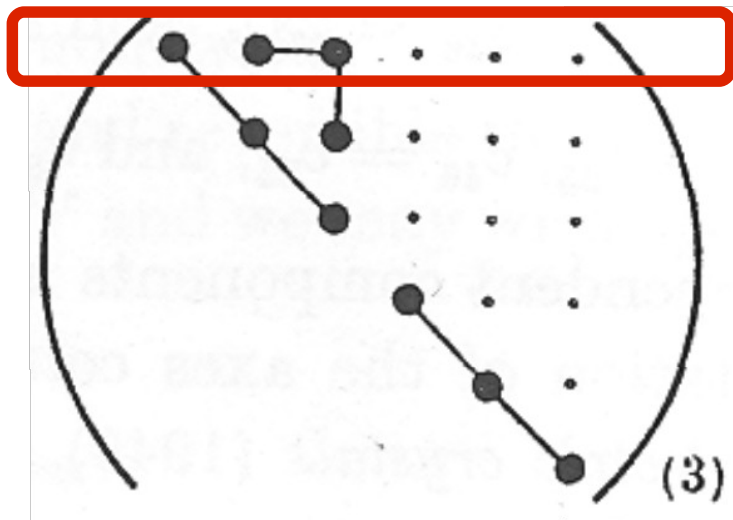


# Elastic Tensor – Clamped Nuclei Term



$$C_{vu}^{\text{ele}} = \frac{1}{V} \frac{f_v|_{\epsilon_u=+\delta} - f_v|_{\epsilon_u=-\delta}}{2\delta}$$

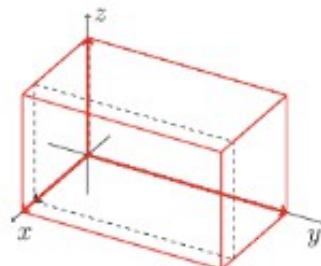
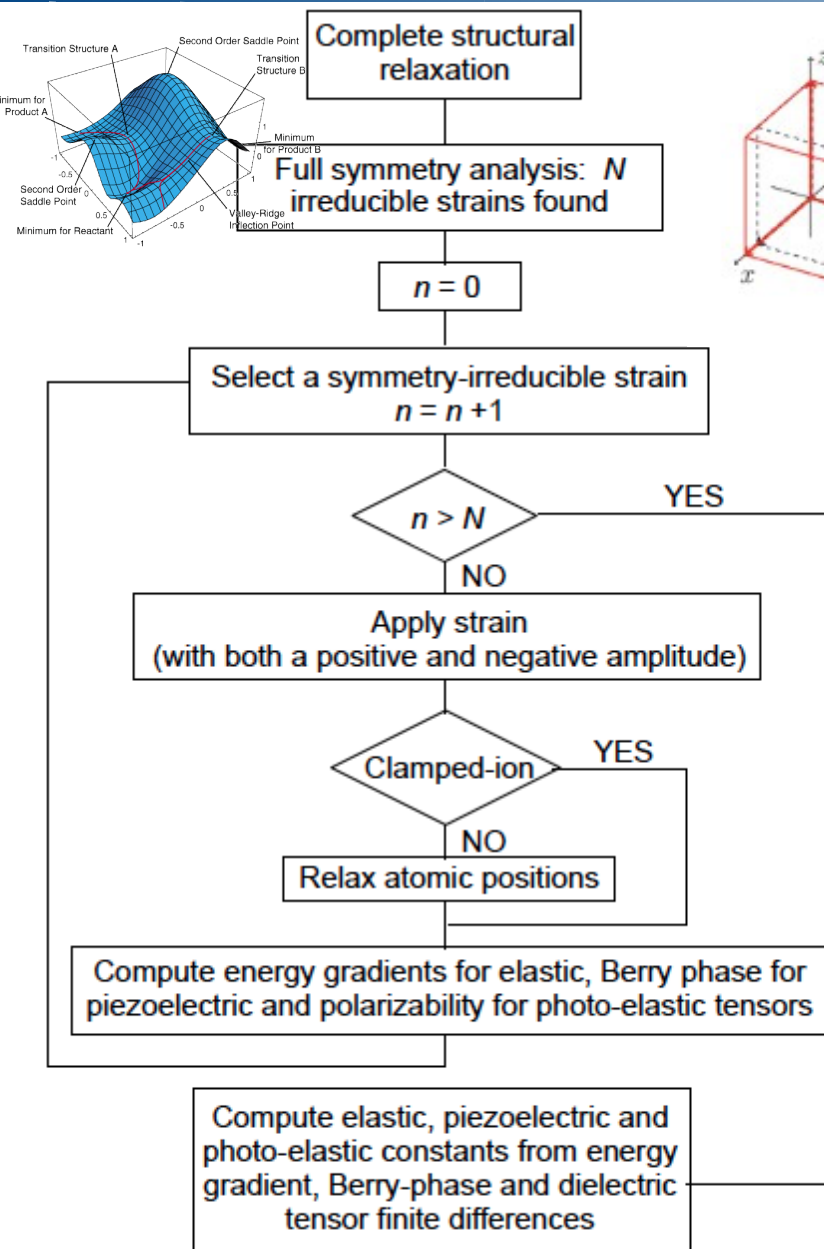
$$C_{11} = C_{12} = C_{13}$$



For a cubic lattice for instance, there are only 2 symmetry-independent strains:  $\epsilon_1$  and  $\epsilon_4$

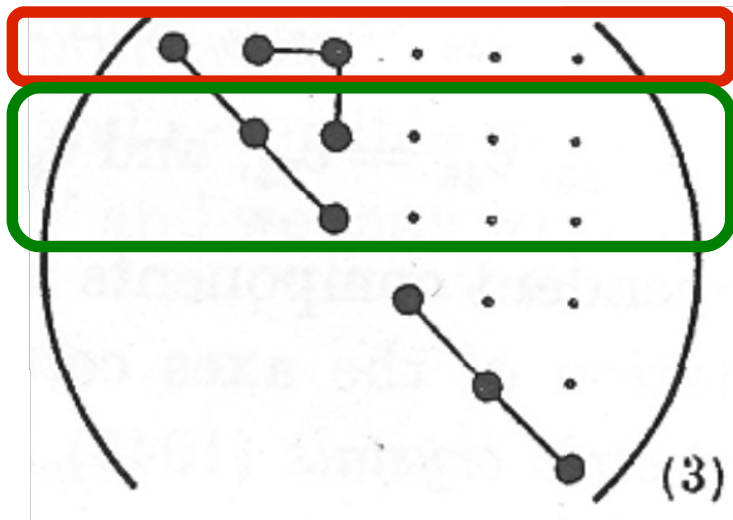


# Elastic Tensor – Clamped Nuclei Term



$$C_{vu}^{\text{ele}} = \frac{1}{V} \frac{f_v|_{\epsilon_u=+\delta} - f_v|_{\epsilon_u=-\delta}}{2\delta}$$

$$C_{11} = C_{12} = C_{13}$$

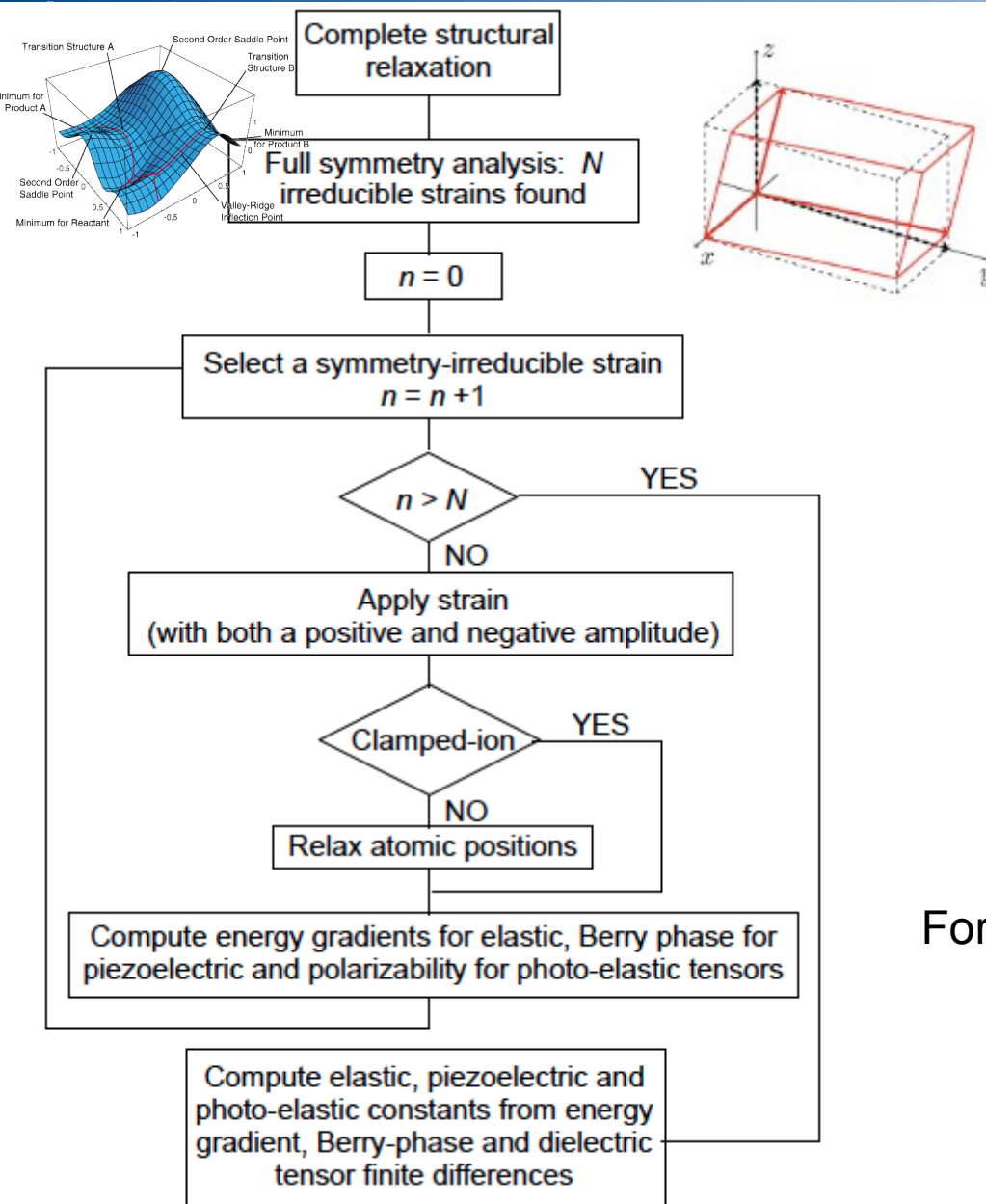


For a cubic lattice for instance, there are only 2 symmetry-independent strains:  $\epsilon_1$  and  $\epsilon_4$

$$C_{11} = C_{22} = C_{33} \text{ and } C_{21} = C_{13}$$

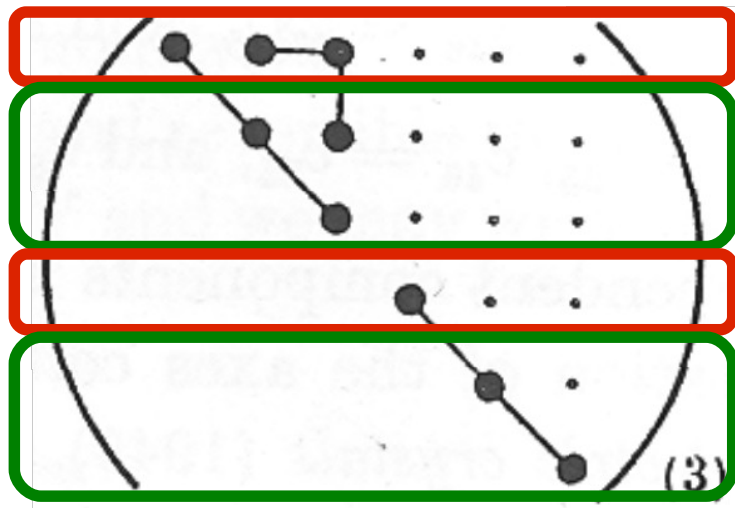


# Elastic Tensor – Clamped Nuclei Term



$$C_{vu}^{\text{ele}} = \frac{1}{V} \frac{f_v|_{\epsilon_u=+\delta} - f_v|_{\epsilon_u=-\delta}}{2\delta}$$

$C_{44}$



For a cubic lattice for instance, there are only 2 symmetry-independent strains:  $\epsilon_1$  and  $\epsilon_4$

$$C_{44} = C_{55} = C_{66}$$



# Elastic Tensor – Nuclear Relaxation

The evaluation of the nuclear relaxation term is generally much more computationally expensive than that of the clamped-nuclei one and, in CRYSTAL, can be achieved following **two alternative approaches**:

- i) performing **geometry optimizations** to relax atomic positions at strained lattice configurations (see flowchart in previous slides);
- ii) computing the **internal-strain tensor** of energy second-derivatives with respect to atomic displacements and lattice deformations, as combined with the harmonic interatomic force constant Hessian matrix.

$$C_{vw} = \frac{1}{V_0} \frac{\partial^2 E}{\partial \eta_v \partial \eta_w} \Big|_{\varepsilon}$$
$$= \frac{1}{V_0} \frac{\partial^2 E}{\partial \eta_v \partial \eta_w} \Big|_{\varepsilon,u} - \frac{1}{V_0} \sum_{ai} A_{ai,v} \Gamma_{ai,w},$$

**Electronic      Nuclear Relax.**

A. Erba, Phys. Chem. Chem. Phys., 18, 13984 (2016)



# Elastic Tensor – Nuclear Relaxation

Where  $\Lambda$  is the **force-response internal-strain tensor**:

$$\Lambda_{ai,v} = \left. \frac{\partial^2 E}{\partial u_{ai} \partial \eta_v} \right|_{\mathcal{E}}.$$

and  $\Gamma$  is the **displacement-response internal-strain tensor**, which describes first-order atomic displacements as induced by a first-order strain:

$$\Gamma_{ai,v} = -\left. \frac{\partial u_{ai}}{\partial \eta_v} \right|_{\mathcal{E}} = \sum_{bj} (H^{-1})_{ai,bj} \Lambda_{bj,v}$$

Where  $\mathbf{H}$  is the **harmonic interatomic force constant Hessian matrix**.

$$H_{ai,bj} = \left. \frac{\partial^2 E}{\partial u_{ai} \partial u_{bj}} \right|_{\mathcal{E},\eta}$$

Diagonalization of  $\mathbf{H}$  allows for a physical partitioning of the nuclear relaxation of the elastic response in terms of zone-center phonons.



# Elastic Tensor – Implementation

In CRYSTAL, there is a fully-automated implementation that allows to compute the elastic tensor of any material in a **single run**.

```
Geometry definition
ELASTCON
[Optional keywords]
END
END
Basis set definition
END
Comput. Parameters
END
```

W.F. Perger, J. Criswell, B. Civalleri, R. Dovesi, Comput. Phys. Commun. 180, 1753-1759 (2009)  
A. Erba, A. Mahmoud, R. Orlando, R. Dovesi, Phys. Chem. Miner. 41, 151-160 (2013)



# Elastic Tensor – Implementation

In CRYSTAL, there is a fully-automated implementation that allows to compute the elastic tensor of any material in a **single run**.

```
Geometry definition
ELASTCON
CLAMPION
END
END
Basis set definition
END
Comput. Parameters
END
```

W.F. Perger, J. Criswell, B. Civalleri, R. Dovesi, Comput. Phys. Commun. 180, 1753-1759 (2009)  
A. Erba, A. Mahmoud, R. Orlando, R. Dovesi, Phys. Chem. Miner. 41, 151-160 (2013)



# Elastic Tensor – Implementation

In CRYSTAL, there is a fully-automated implementation that allows to compute the elastic tensor of any material in a **single run**.

```
Geometry definition
ELASTCON
PREOPTGEOM
END
END
Basis set definition
END
Comput. Parameters
END
```

W.F. Perger, J. Criswell, B. Civalleri, R. Dovesi, Comput. Phys. Commun. 180, 1753-1759 (2009)  
A. Erba, A. Mahmoud, R. Orlando, R. Dovesi, Phys. Chem. Miner. 41, 151-160 (2013)



# Elastic Tensor – Born Stability Criteria

The **Born stability criteria** are fundamental conditions for determining if a crystalline solid is mechanically stable, requiring its elastic energy to be a positive definite quadratic form, meaning any small strain increases the free energy, ensuring the crystal doesn't spontaneously deform or collapse.

For unstressed crystals, this translates to the **elastic constant matrix having positive eigenvalues** (or positive leading principal minors, known as Sylvester's criterion).

**Cubic**

$$\begin{pmatrix} C_{11} & C_{12} & C_{12} \\ C_{12} & C_{11} & C_{12} \\ C_{12} & C_{12} & C_{11} \end{pmatrix} = \begin{pmatrix} C_{44} & & \\ & C_{44} & \\ & & C_{44} \end{pmatrix}$$

$$C_{11} - C_{12} > 0; \quad C_{11} + 2C_{12} > 0; \quad C_{44} > 0$$

**Hexagonal**

$$\begin{pmatrix} C_{11} & C_{12} & C_{13} \\ C_{12} & C_{11} & C_{13} \\ C_{13} & C_{13} & C_{33} \end{pmatrix} = \begin{pmatrix} C_{44} & & \\ & C_{44} & \\ & & C_{66} \end{pmatrix}$$

$$C_{11} > |C_{12}|; \quad 2C_{13}^2 < C_{33}(C_{11} + C_{12}); \\ C_{44} > 0; \quad C_{66} > 0$$

**Orthorhombic**

$$\begin{pmatrix} C_{11} & C_{12} & C_{13} \\ C_{12} & C_{22} & C_{23} \\ C_{13} & C_{23} & C_{33} \end{pmatrix} = \begin{pmatrix} C_{44} & & \\ & C_{55} & \\ & & C_{66} \end{pmatrix}$$

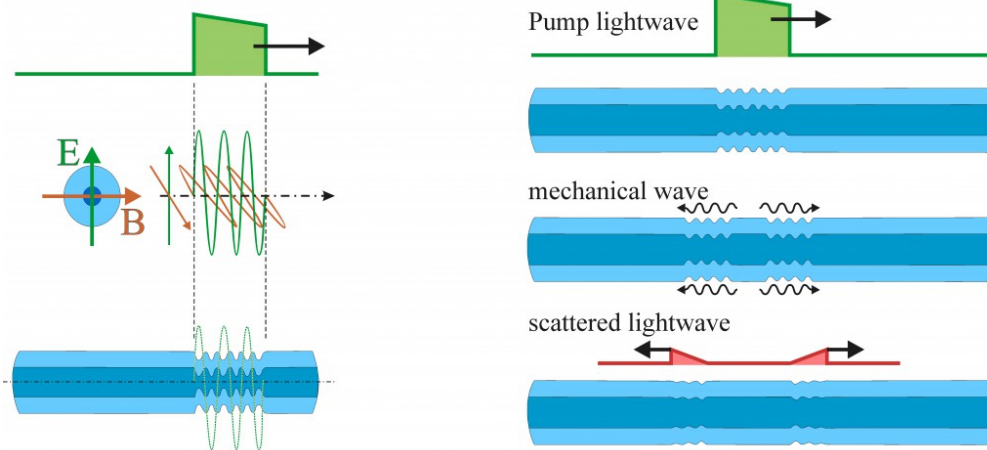
$$C_{11} > 0; \quad C_{11}C_{22} > C_{12}^2; \\ C_{11}C_{22}C_{33} + 2C_{12}C_{13}C_{23} - C_{11}C_{23}^2 - C_{33}C_{12}^2 > 0 \\ C_{44} > 0; \quad C_{55} > 0; \quad C_{66} > 0$$

In CRYSTAL, these conditions are checked.



# Elastic Wave Velocities

Experimentally, elastic constants are determined via **Brillouin scattering** measurements.



The primary observable quantities are **elastic (acoustic, seismic) wave velocities**. The **Christoffel equation** is a fundamental concept in continuum mechanics and wave physics, especially for anisotropic materials like crystals, describing how acoustic waves (sound, elastic waves) propagate by relating wave velocity and polarization to the material's elastic properties and density, often solved as an **eigenvalue problem** to find wave speeds and directions.

$$\mathbf{A}^{\hat{\mathbf{q}}}\mathbf{U} = \mathbf{V}^2\mathbf{U} \quad \text{with} \quad A_{jk}^{\hat{\mathbf{q}}} = \frac{1}{\rho} \sum_{il} \hat{q}_i C_{ijkl} \hat{q}_l,$$

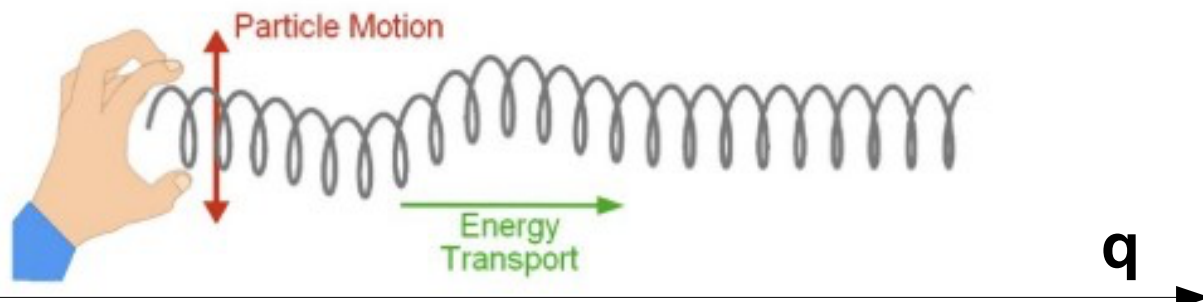


# Elastic Wave Velocities

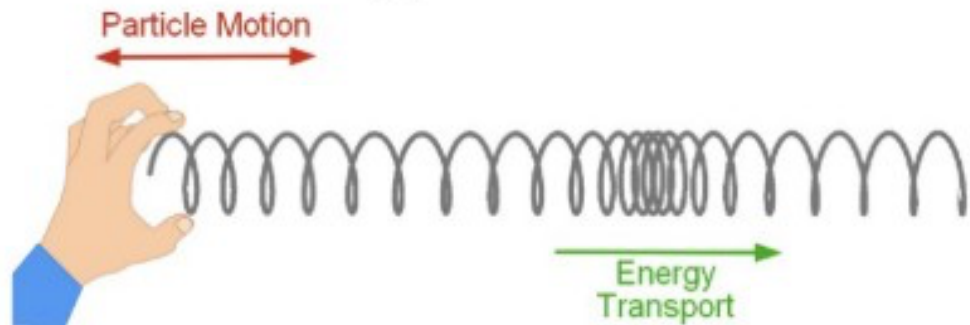
For a given propagation direction  $\mathbf{q}$  in the lattice, there are 3 possible wave polarizations: **1 longitudinal** and **2 transverse**.

$$\mathbf{A}^{\hat{\mathbf{q}}} \mathbf{U} = \mathbf{V}^2 \mathbf{U}$$

## Transverse



## Longitudinal

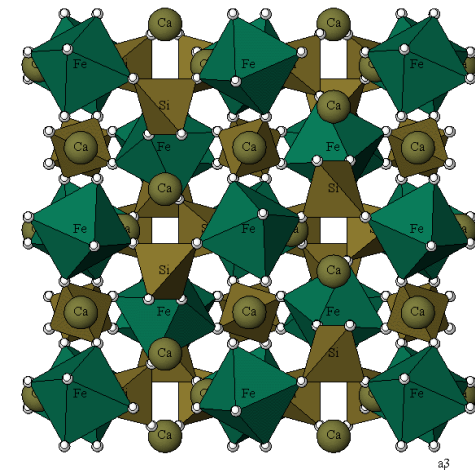
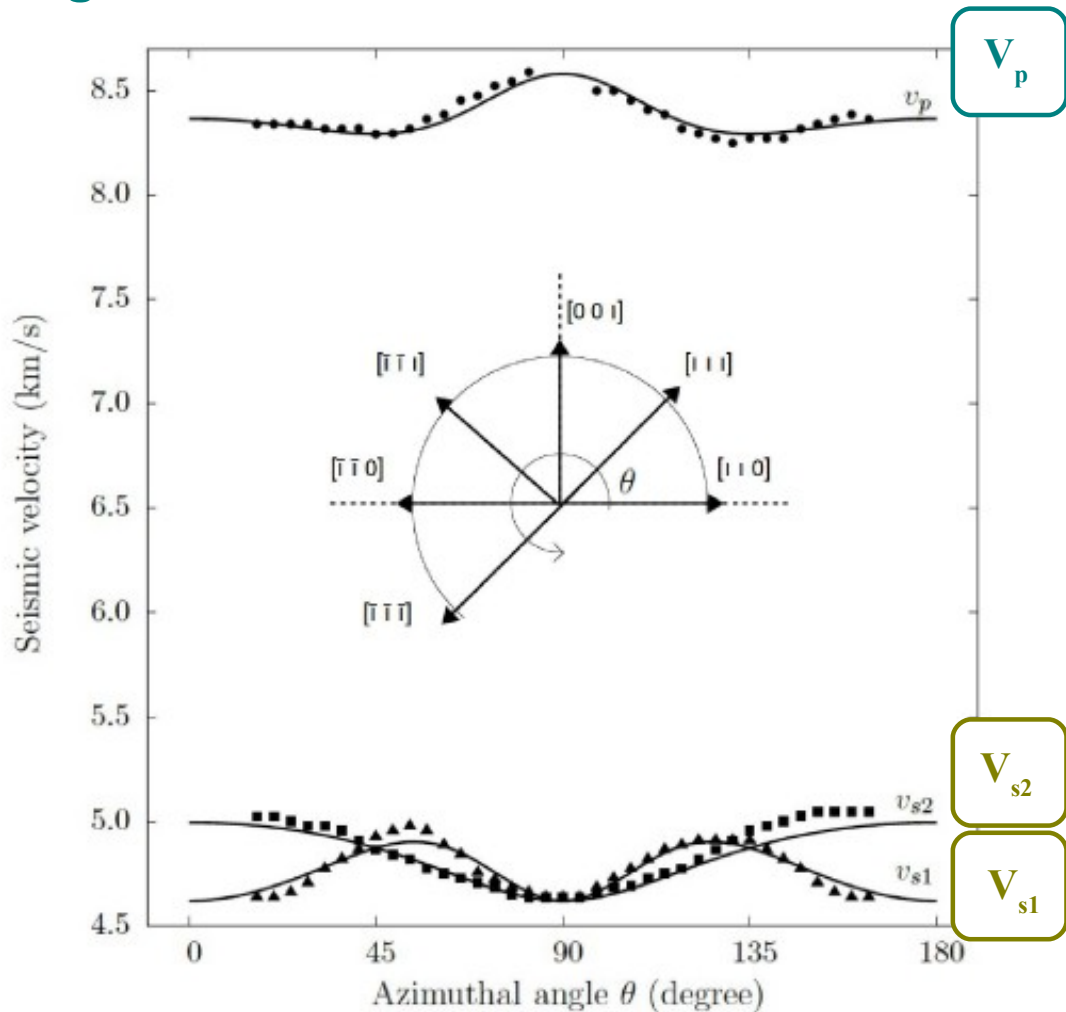




# Elastic Wave Velocities

For a given propagation direction  $\mathbf{q}$  in the lattice, there are 3 possible wave polarizations: **1 longitudinal** and **2 transverse**.

$$\mathbf{A}^{\hat{\mathbf{q}}}\mathbf{U} = \mathbf{V}^2\mathbf{U}$$



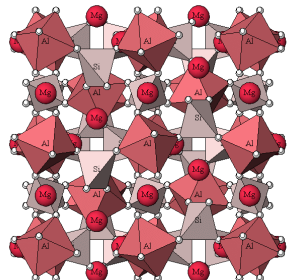
Andradite

Experimental data from single-crystal Brillouin scattering measurements by Jiang *et al.*, *J. Phys.: Condens. Matter*, **16**, S1041 (2004)

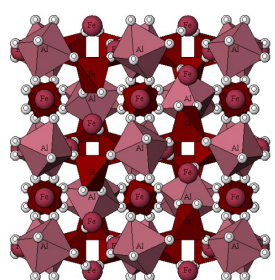


# Elastic Wave Velocities

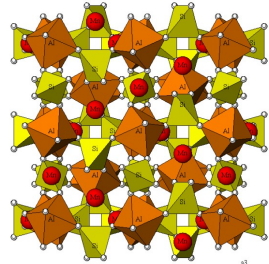
For a given propagation direction  $\mathbf{q}$  in the lattice, there are 3 possible wave polarizations: **1 longitudinal** and **2 transverse**.



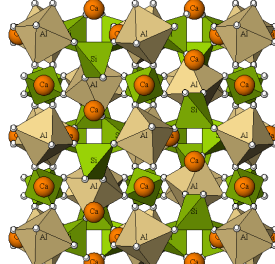
Pyrope



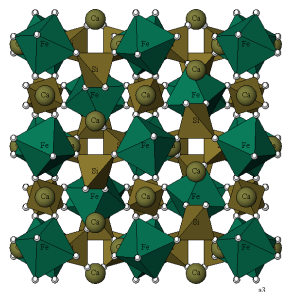
Almandine



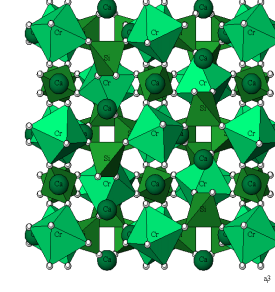
Spessartine



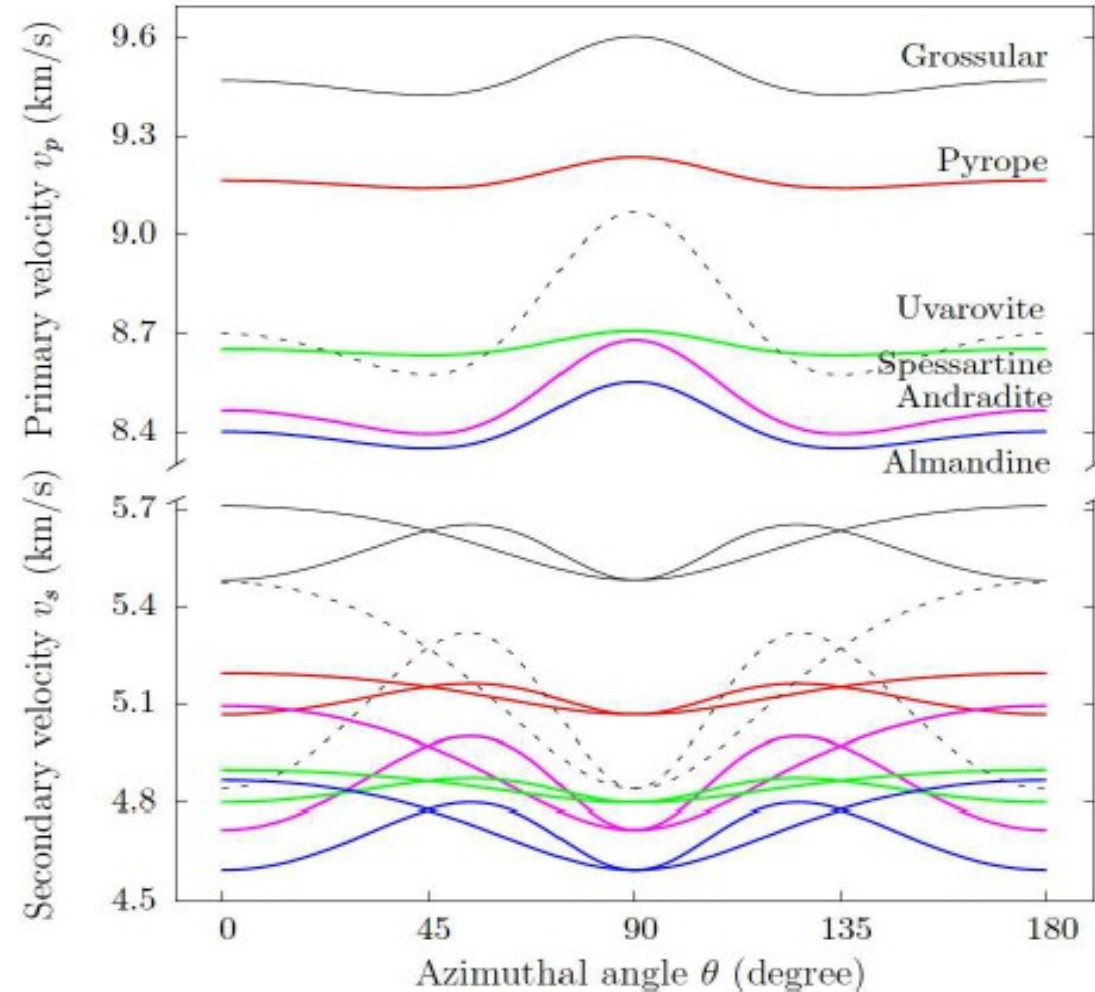
Grossular



Andradite



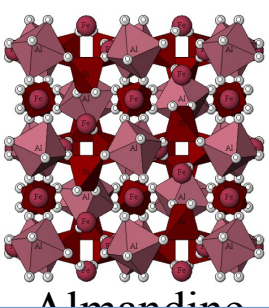
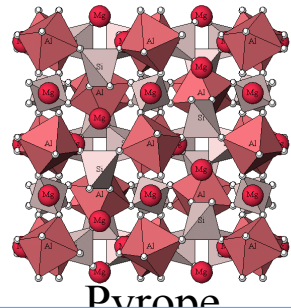
Uvarovite





# Elastic Wave Velocities

For a given propagation direction  $\mathbf{q}$  in the lattice, there are 3 possible wave polarizations: **1 longitudinal** and **2 transverse**.



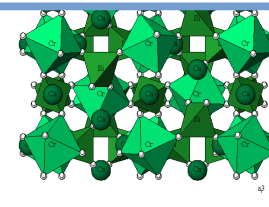
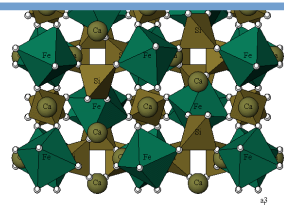
## Elastic Anisotropy

$\text{Spe} < \text{Pyr} < \text{Gro} < \text{Alm} < \text{And} \ll \text{Uva}$

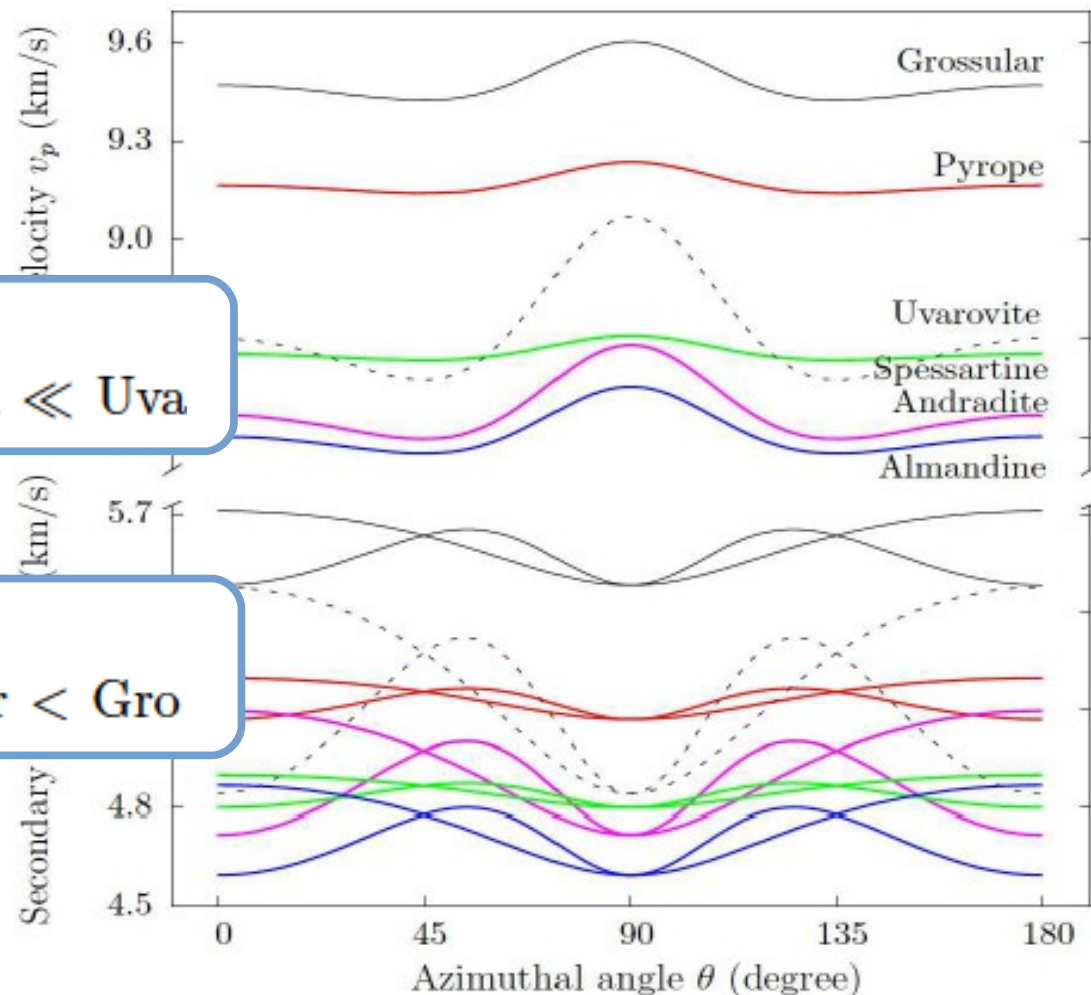


## Seismic wave velocity

$\text{Alm} < \text{And} < \text{Spe} < \text{Uva} < \text{Pyr} < \text{Gro}$



Andradite





# Elastic Wave Velocities

The **AWESoMe** program has been merged into CRYSTAL and can now be used as a keyword (**AWESOME**) of the **ELASTCON** input block. The code computes the **phase and group velocities** for many propagation directions, as well as some related parameters such as the **polarization vectors**, the **power flow angle** and the **enhancement factor**.

=====  
A W E S O M E  
=====  
Acoustic  
Wave  
Evaluator in  
Solid  
Media

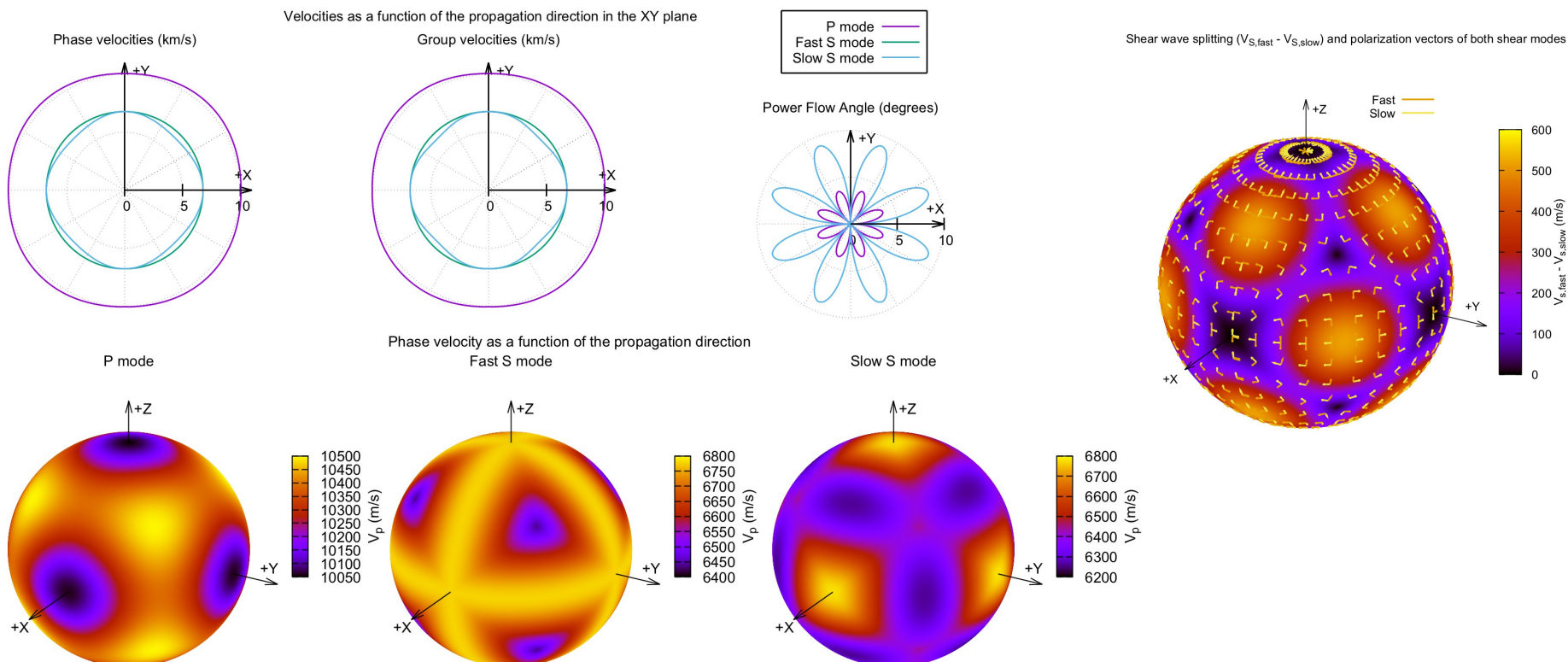
D. Munoz-Santiburcio, A. Hernandez-Laguna and J.I. Soto, *Comp. Phys. Commun.*, **192**, 272-277 (2015)

A. Erba QMMC2026 Volta Redonda – Rio de Janeiro, Brazil, January 2026



# Elastic Wave Velocities

The **AWESoMe** program has been merged into CRYSTAL and can now be used as a keyword (**AWESOME**) of the **ELASTCON** input block. The code computes the **phase and group velocities** for many propagation directions, as well as some related parameters such as the **polarization vectors**, the **power flow angle** and the **enhancement factor**.



D. Munoz-Santiburcio, A. Hernandez-Laguna and J.I. Soto, *Comp. Phys. Commun.*, **192**, 272-277 (2015)

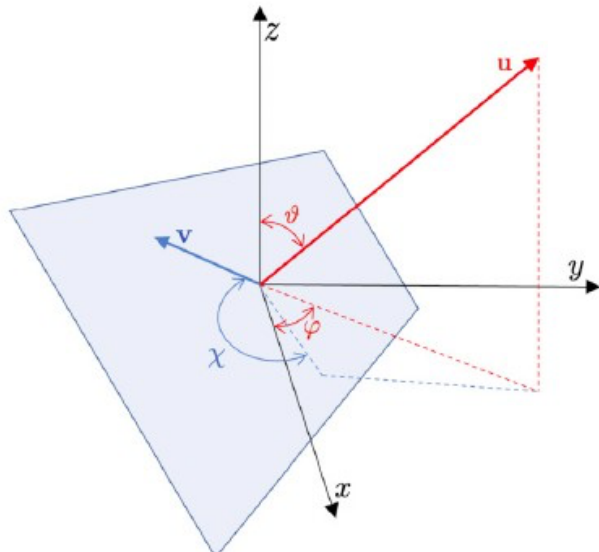


# Elastic Properties

A variety of elastic properties can be derived from the elastic tensor  $\mathbf{C}$ , including **bulk modulus**, **shear modulus**, **Young's modulus**, **Poisson's ratio**.

A)

$$\mathbf{u} = \begin{pmatrix} \sin \vartheta \cos \varphi \\ \sin \vartheta \sin \varphi \\ \cos \vartheta \end{pmatrix}$$



$$\mathbf{v} = \begin{pmatrix} \cos \vartheta \cos \varphi \cos \chi - \sin \varphi \sin \chi \\ \cos \vartheta \sin \varphi \cos \chi + \cos \varphi \sin \chi \\ -\sin \vartheta \cos \chi \end{pmatrix}$$

The directional **Young modulus  $E$**  (i.e. the strain response of a solid to an uniaxial stress, in the direction of the stress):

$$E(\vartheta, \varphi) = \frac{1}{u_i u_j u_k u_l S_{ijkl}} \quad \text{where} \quad \mathbf{S} = \mathbf{C}^{-1}$$

The directional **linear compressibility  $\beta$**  (i.e. the linear strain under the application of an external hydrostatic stress):

$$\beta(\vartheta, \varphi) = S_{ijkk} u_i u_j$$

The **shear modulus  $G$**  (i.e. the strain response to a shear stress):

$$G(\vartheta, \varphi, \chi) = \frac{1}{u_i v_j u_k v_l S_{ijkl}}$$

The **Poisson's ratio  $\nu$**  (i.e. the strain response in the directions orthogonal to a uniaxial stress):

$$\nu(\vartheta, \varphi, \chi) = -\frac{u_i u_j v_k v_l S_{ijkl}}{u_i u_j u_k u_l S_{ijkl}}$$

The first two quantities depend on a single direction  $\mathbf{u}$  (and thus on two angles  $\vartheta$  and  $\phi$  in spherical coordinates), whereas, the latter two depend on two directions  $\mathbf{u}$  and  $\mathbf{v}$  (if orthogonal, the two directions can be defined in terms of three angles  $\vartheta$ ,  $\phi$ , and  $\chi$  in spherical coordinates). Einstein's notation is implied.

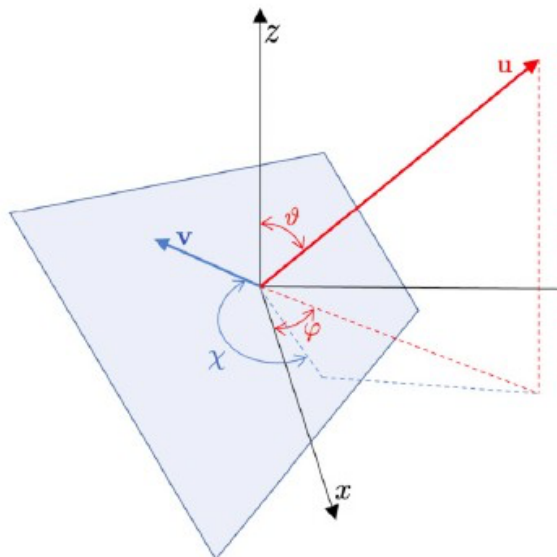


# Elastic Properties

A variety of elastic properties can be derived from the elastic tensor  $\mathbf{C}$ , including **bulk modulus, shear modulus, Young's modulus, Poisson's ratio**.

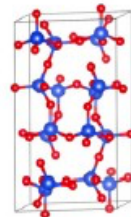
A)

$$\mathbf{u} = \begin{pmatrix} \sin \vartheta \cos \varphi \\ \sin \vartheta \sin \varphi \\ \cos \vartheta \end{pmatrix}$$

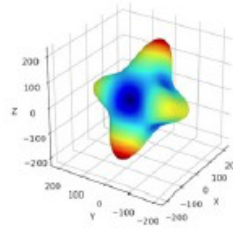


B)

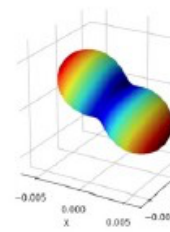
Coesite



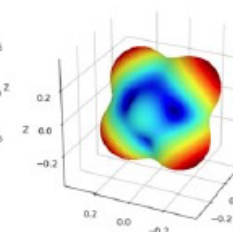
$E(\vartheta, \varphi)$



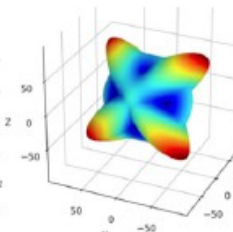
$\beta(\vartheta, \varphi)$



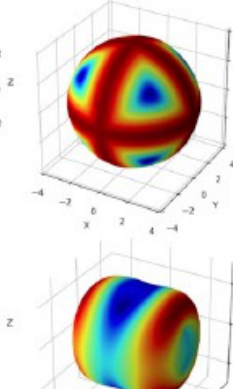
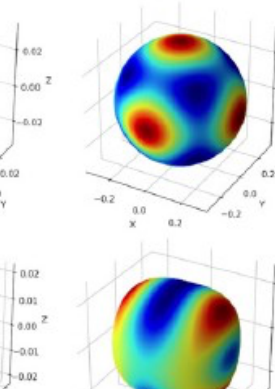
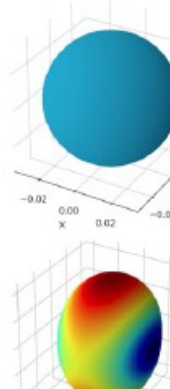
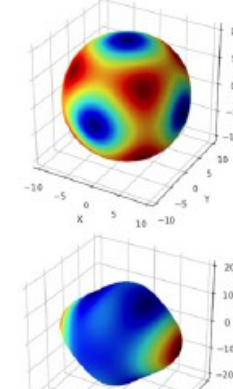
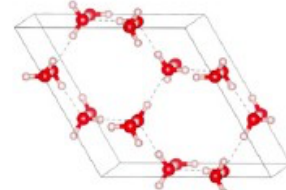
$G_{\text{avg}}(\vartheta, \varphi, \chi)$



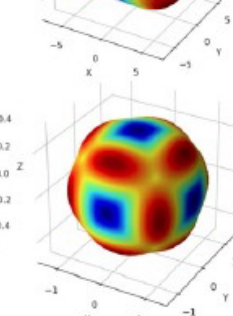
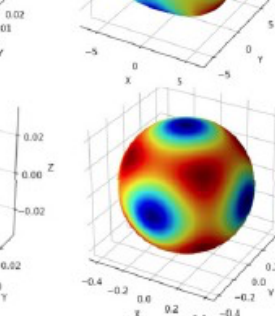
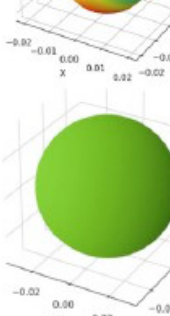
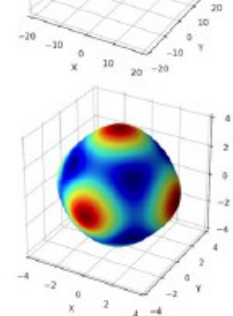
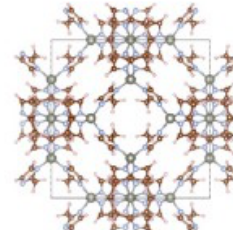
$\nu_{\max}(\vartheta, \varphi, \chi)$



Ice XI



ZIF-8

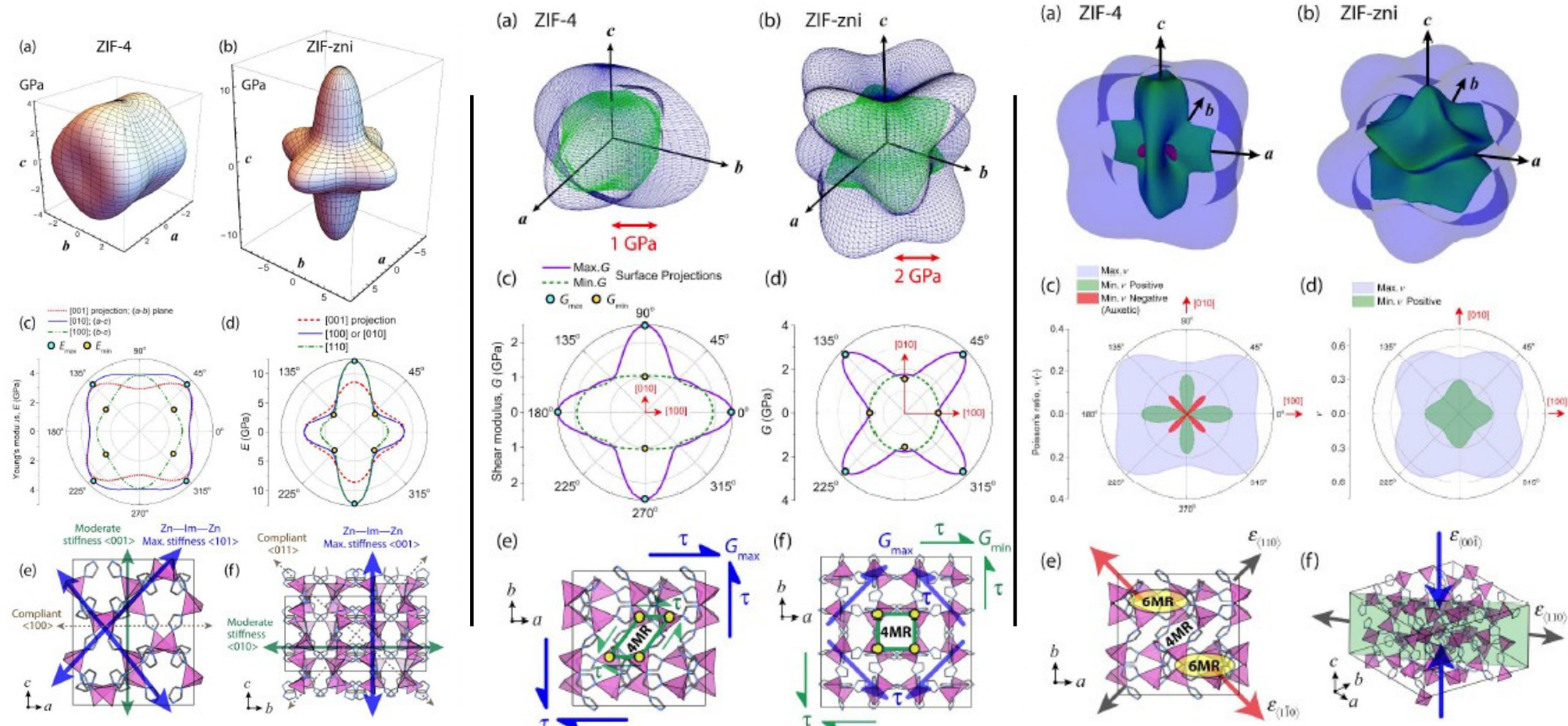


B. Camino, ..., A. Erba, N. Harrison, Comput. Phys. Commun., 292, 108853 (2023)



# Elastic Properties

A variety of elastic properties can be derived from the elastic tensor  $\mathbf{C}$ , including **bulk modulus**, **shear modulus**, **Young's modulus**, **Poisson's ratio**.

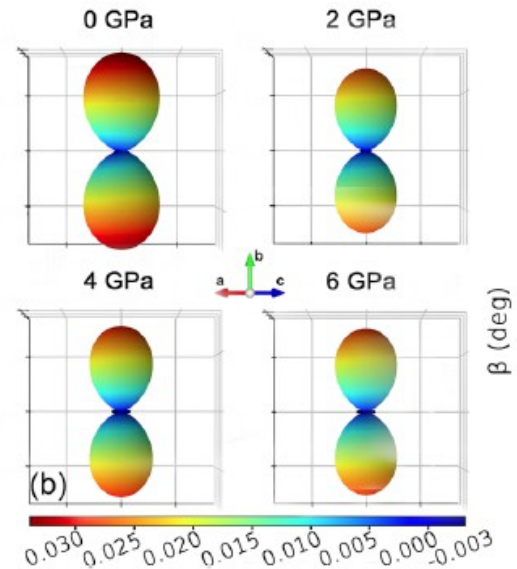
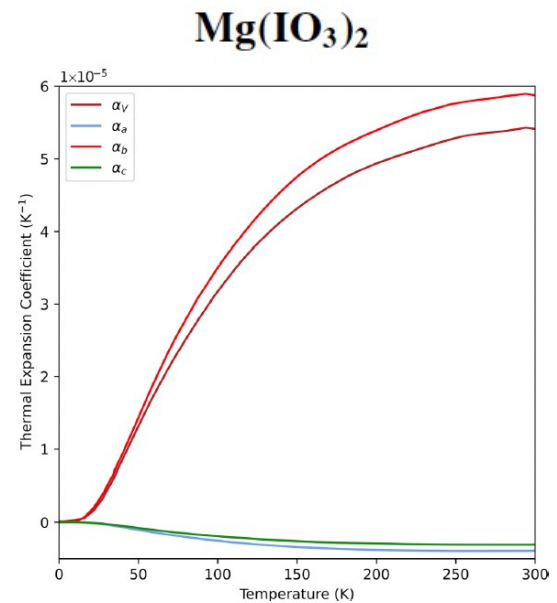
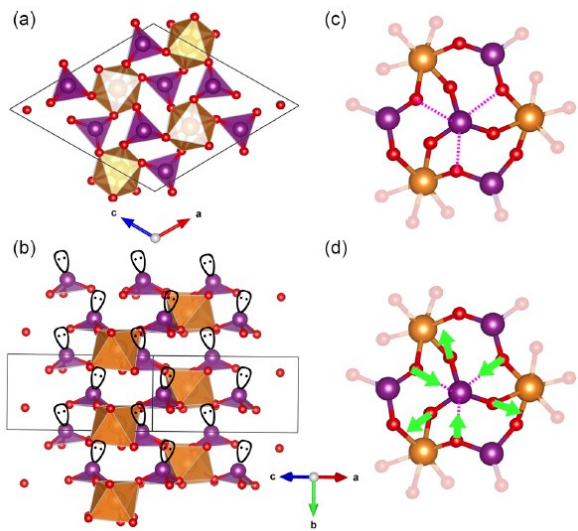


J. Tan, B. Civalleri, A. Erba, E. Albanese, CrystEngComm, 17, 375-382 (2015)



# Elastic Properties

A variety of elastic properties can be derived from the elastic tensor  $\mathbf{C}$ , including **bulk modulus, shear modulus, Young's modulus, Poisson's ratio**.



**Negative linear compressibility and phonon softening in Mg(IO<sub>3</sub>)<sub>2</sub> under pressure**

F. Bodo, E. Kraka, A. Erba, Phys. Rev. B, 113, 024107 (2026)

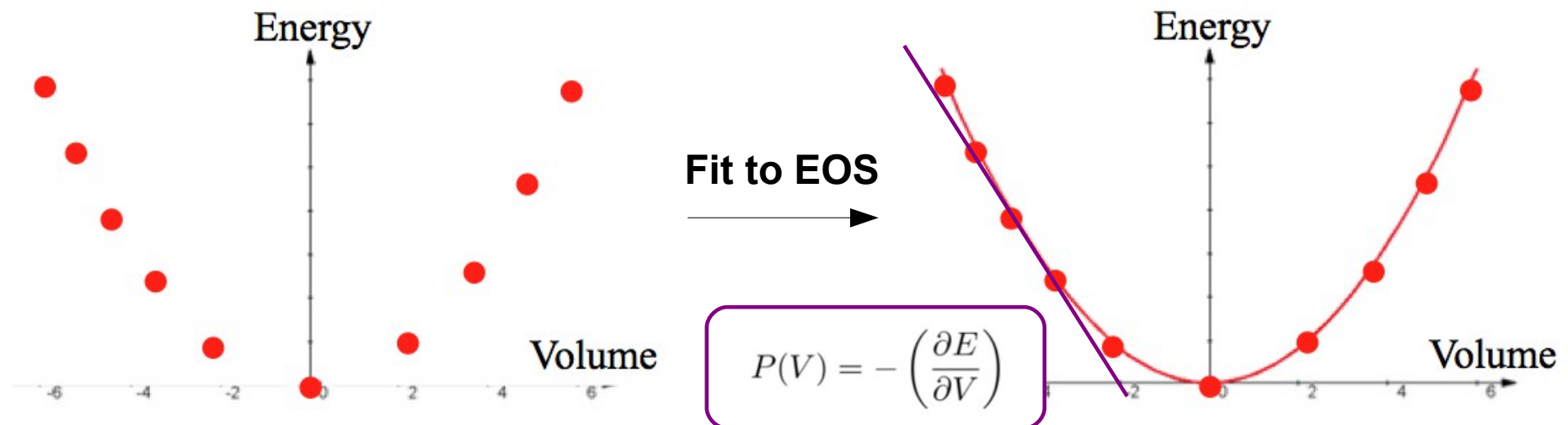


# Elastic Tensor under Pressure

To compute the elastic response of a material at a given pressure  $P$ , as a preliminary step one has to determine the equilibrium structure at  $P$ . In CRYSTAL, it can be done with:

- 1) **pressure-constrained geometry optimization**, via a hydrostatic pre-stress.
- 2) **equation-of-state (EOS) approach** through volume-constrained optimizations.

In EOS, constant-volume optimizations are performed at different volumes to get a  $E(V)$  curve that is then fitted to evaluate the slope (**pressure**) and curvature (**bulk modulus**).





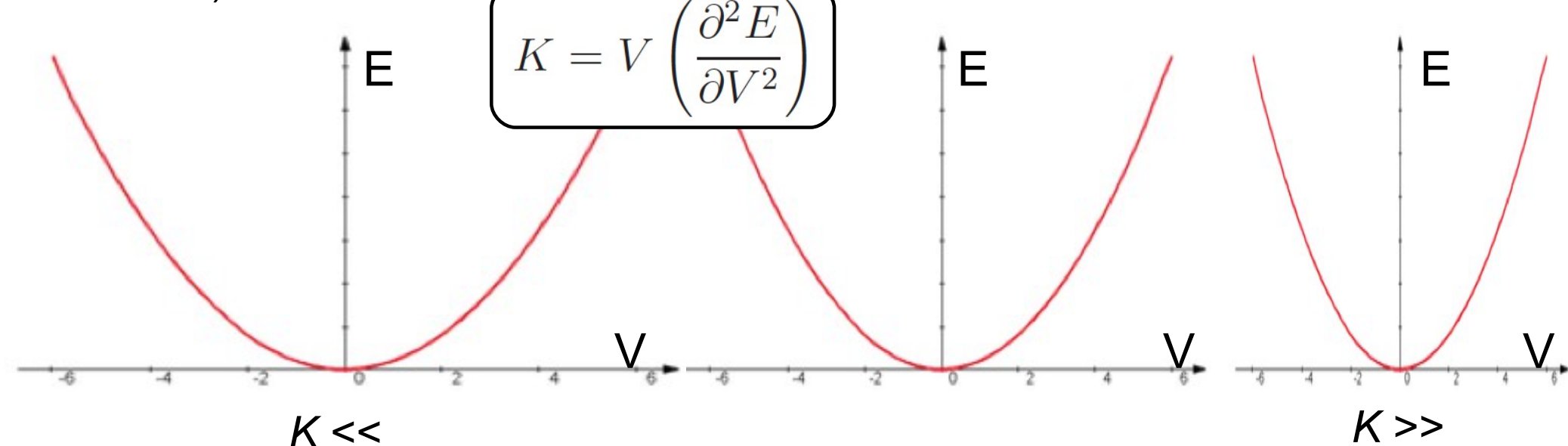
# Elastic Tensor under Pressure

To compute the elastic response of a material at a given pressure  $P$ , as a preliminary step one has to determine the equilibrium structure at  $P$ . In CRYSTAL, it can be done with:

- 1) **pressure-constrained geometry optimization**, via a hydrostatic pre-stress.
- 2) **equation-of-state (EOS) approach** through volume-constrained optimizations.

In EOS, constant-volume optimizations are performed at different volumes to get a  $E(V)$  curve that is then fitted to evaluate the slope (**pressure**) and curvature (**bulk modulus**).

$$K = V \left( \frac{\partial^2 E}{\partial V^2} \right)$$





# Elastic Tensor under Pressure

To compute the elastic response of a material at a given pressure  $P$ , as a preliminary step one has to determine the equilibrium structure at  $P$ . In CRYSTAL, it can be done with:

- 1) pressure-constrained geometry optimization**, via a hydrostatic pre-stress.
- 2) equation-of-state (EOS) approach** through volume-constrained optimizations.

Once the equilibrium lattice configuration under a hydrostatic pressure is determined, elastic stiffness constants can be computed as:

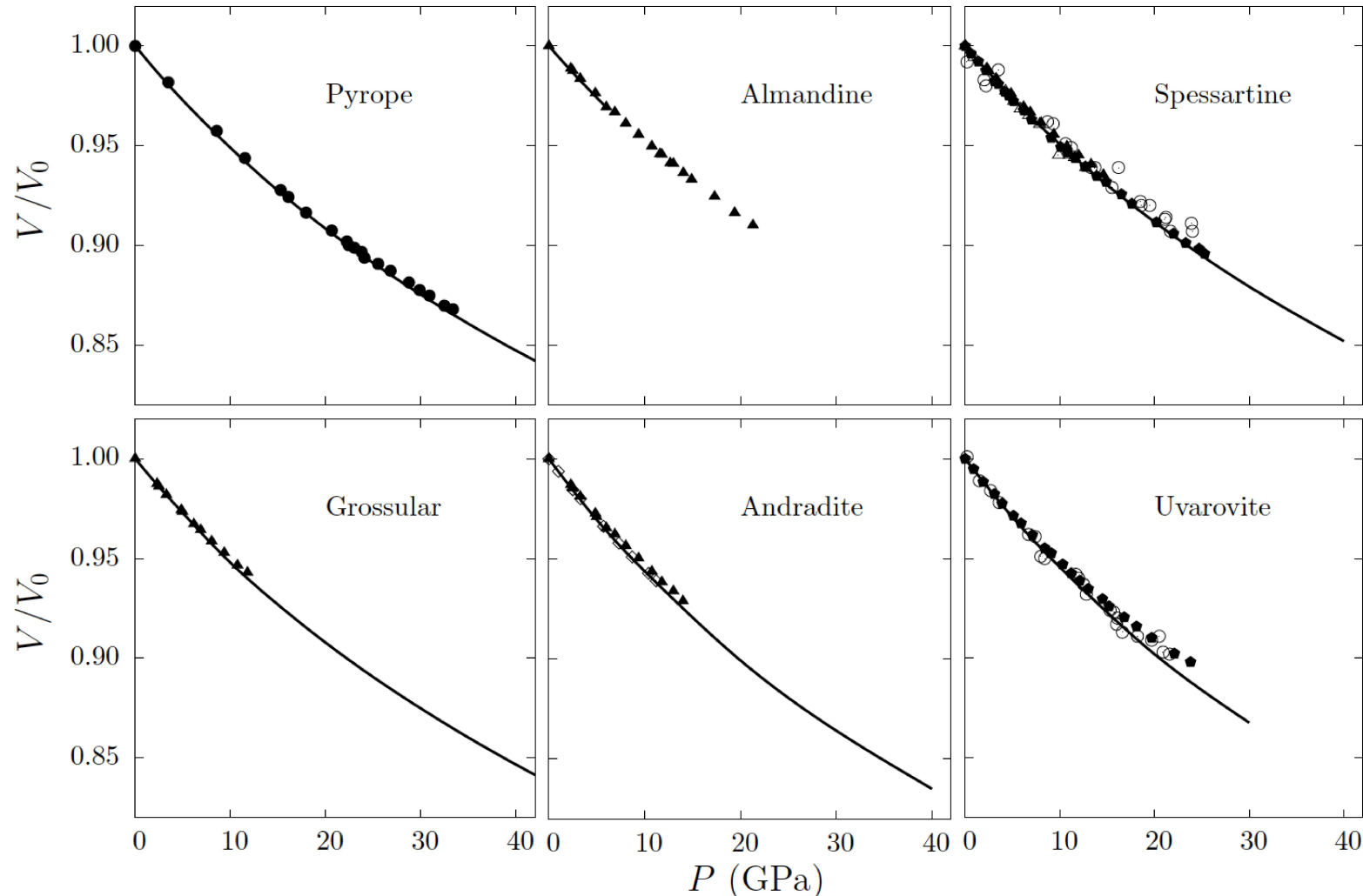
$$C_{ijkl}(P) = \frac{1}{V(P)} \left. \frac{\partial^2 E}{\partial \epsilon_{ij} \partial \epsilon_{kl}} \right|_P + \frac{P}{2} (2\delta_{ij}\delta_{kl} - \delta_{il}\delta_{jk} - \delta_{ik}\delta_{jl})$$

A. Erba, A. Mahmoud, D. Belmonte and R. Dovesi, J. Chem. Phys., 140, 124703 (2014)



# Elastic Tensor under Pressure

Some results on silicate garnets:

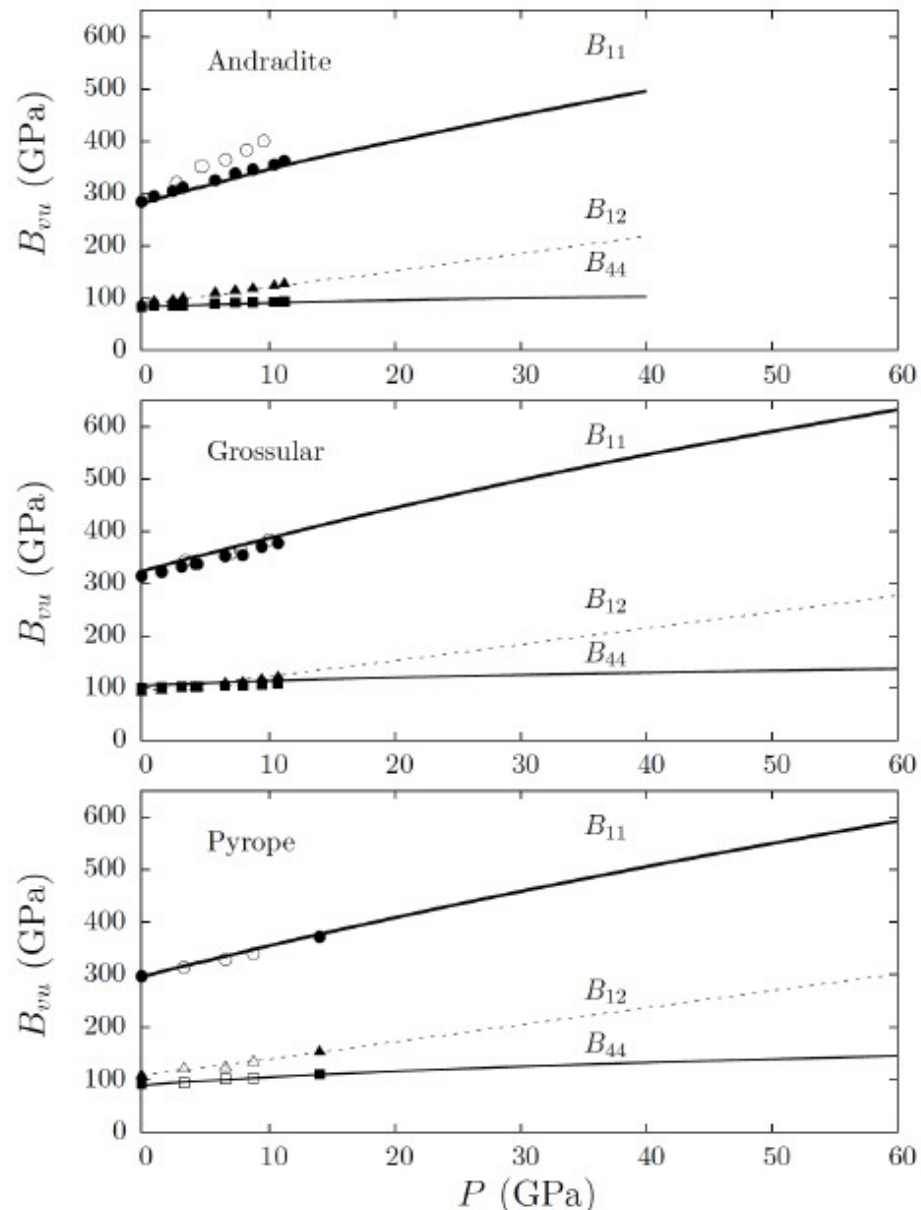
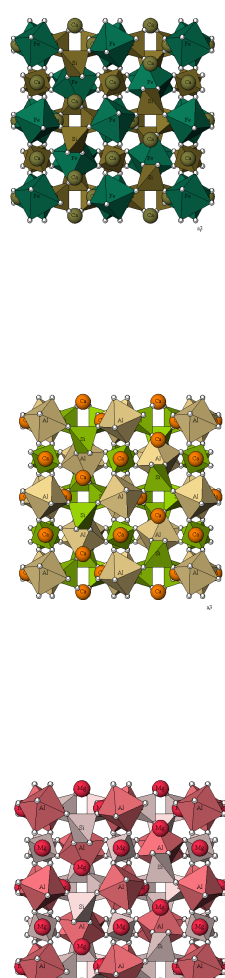
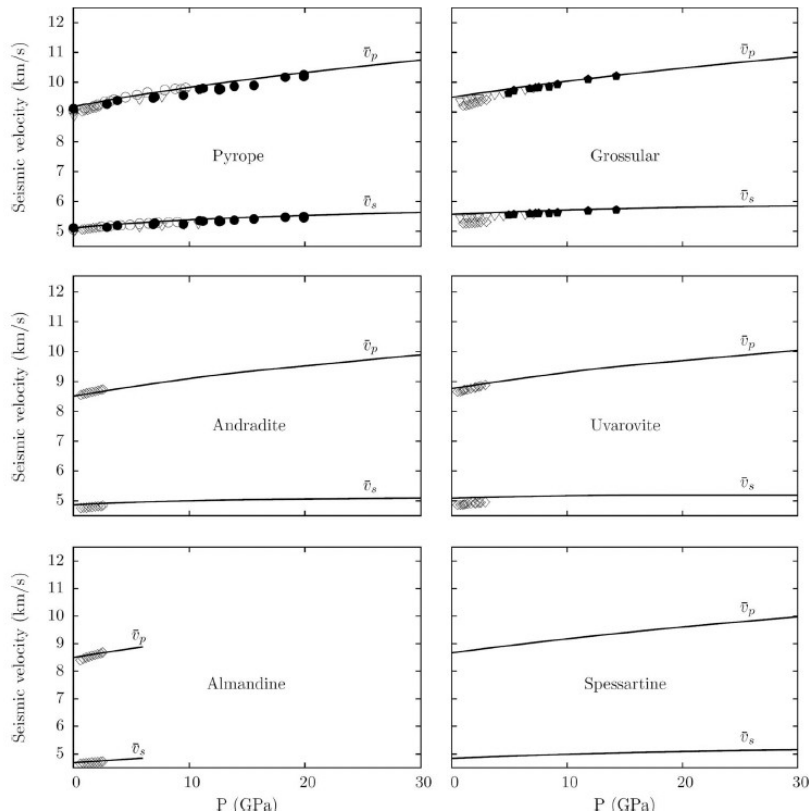


A. Erba, A. Mahmoud, D. Belmonte and R. Dovesi, J. Chem. Phys., 140, 124703 (2014)



# Elastic Tensor under Pressure

Some results on silicate garnets:

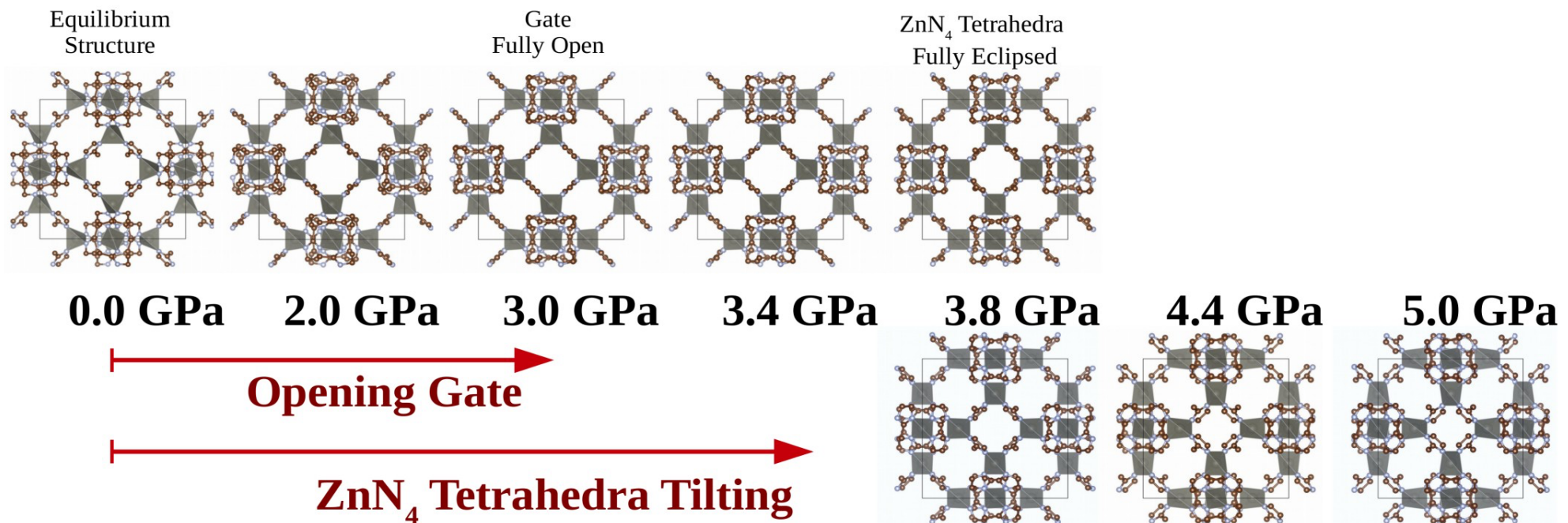


A. Mahmoud, A. Erba, K. Doll, R. Dovesi  
J. Chem. Phys. 140, 234703 (2014)



# Elastic Tensor under Pressure

Some results on ZIF-8, through a pressure-induced first-order phase transition.

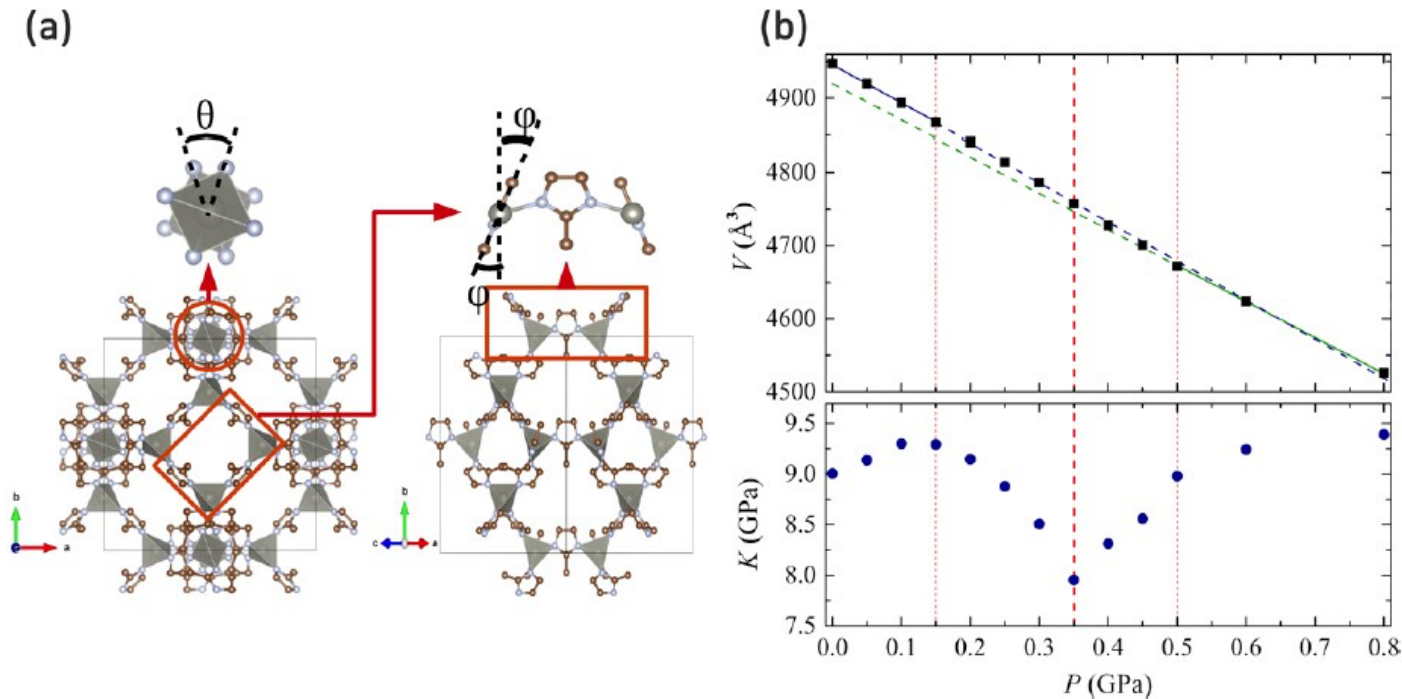


W. Zhang, ..., A. Erba, M.T. Ruggiero, J. Phys. Chem. C, 122, 27442–27450 (2018)



# Elastic Tensor under Pressure

Some results on ZIF-8, through a pressure-induced first-order phase transition.

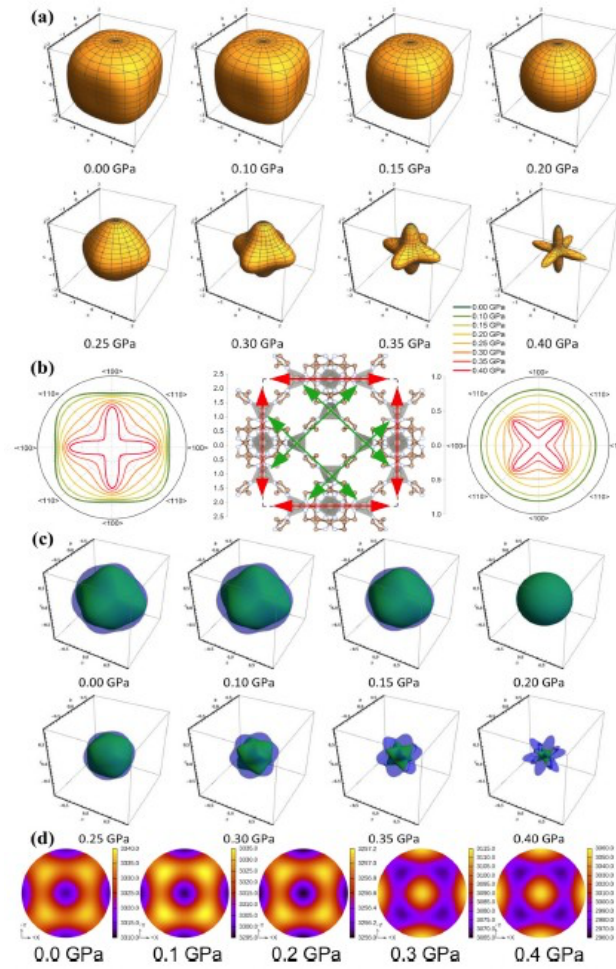
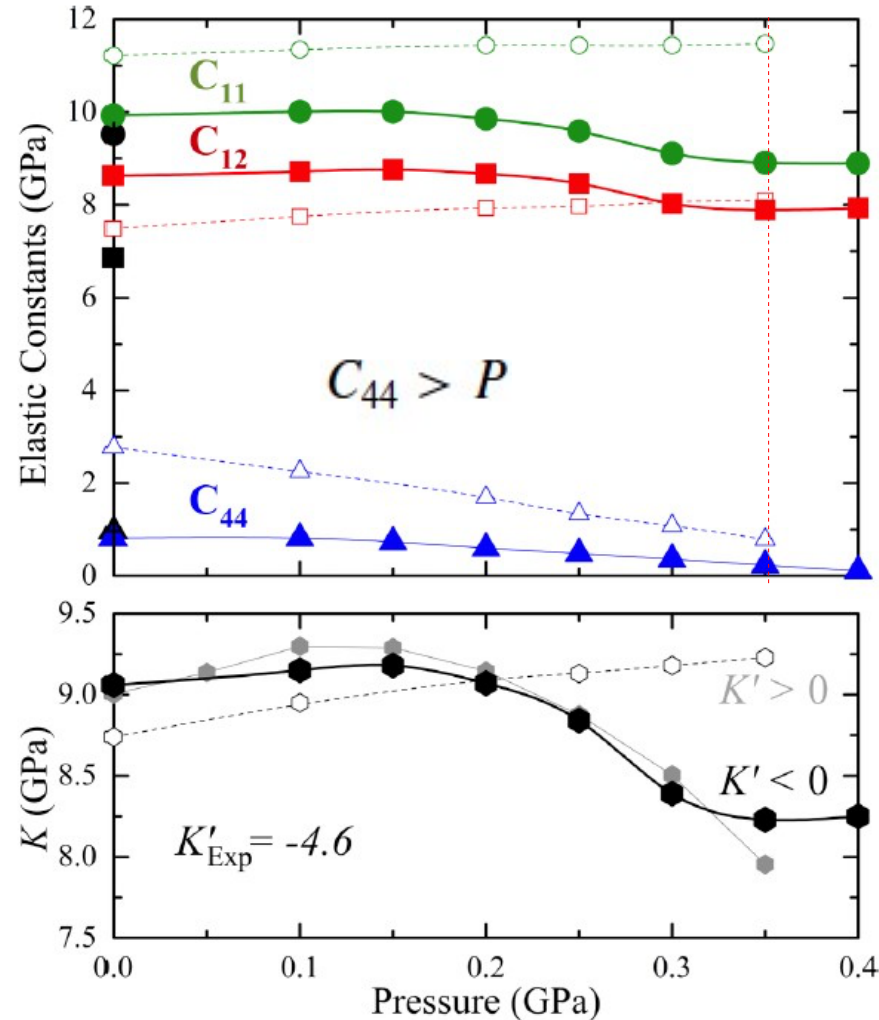


W. Zhang, ..., A. Erba, M.T. Ruggiero, J. Phys. Chem. C, 122, 27442–27450 (2018)



# Elastic Tensor under Pressure

Some results on ZIF-8, through a pressure-induced first-order **phase transition**, with a **shear-destabilization** eventually leading to amorphization.

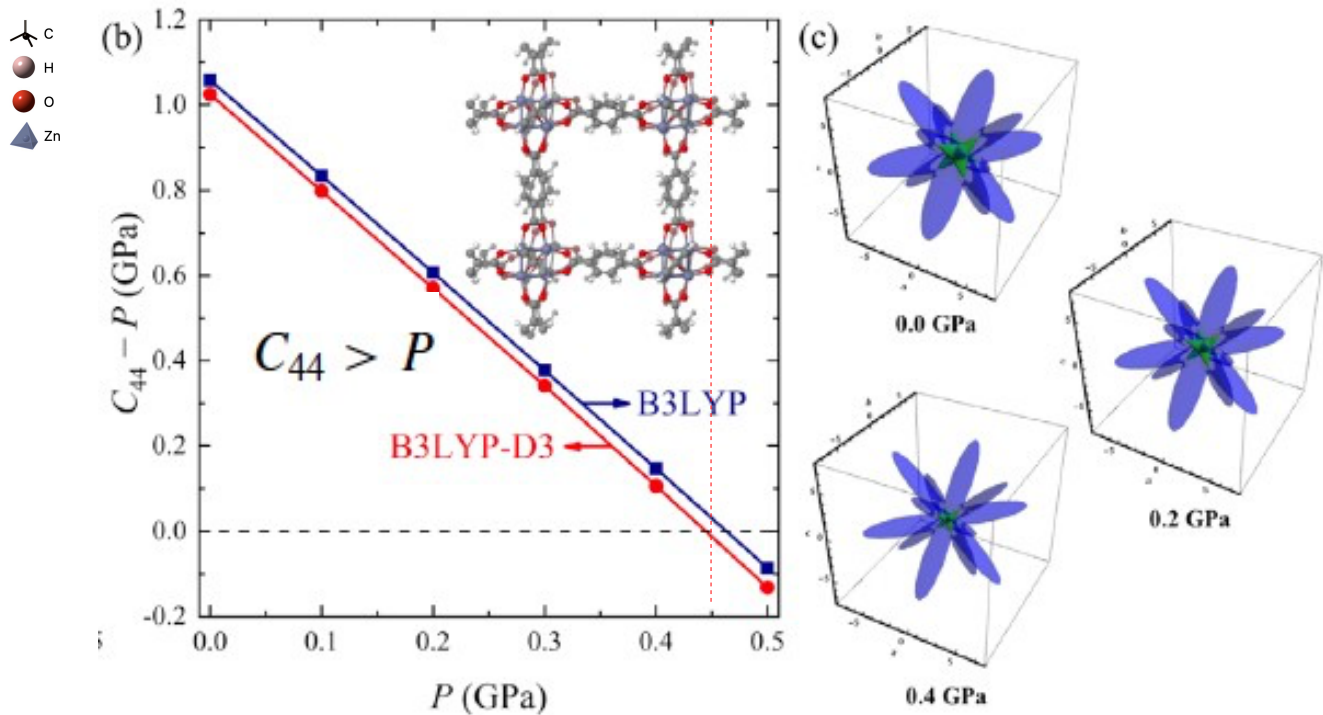
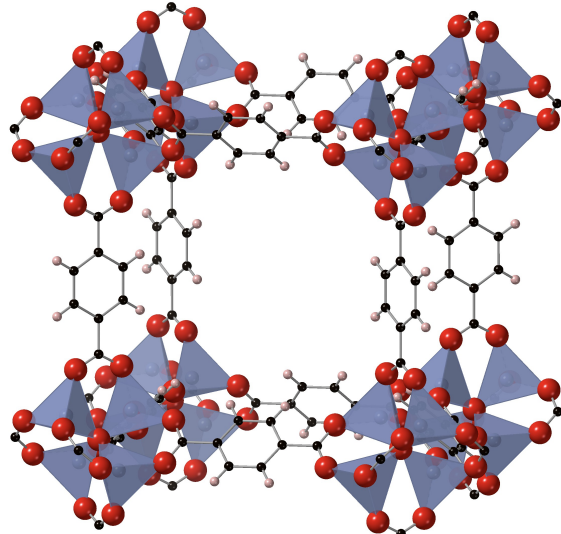


J. Maul, M. Ryder, M.T. Ruggiero, A. Erba, Phys. Rev. B, 99, 014102 (2019)



# Elastic Tensor under Pressure

Some results on MOF-5:



M. Ryder, J. Maul, B. Civalleri, A. Erba, Adv. Theory Simul., 2, 1900093 (2019)

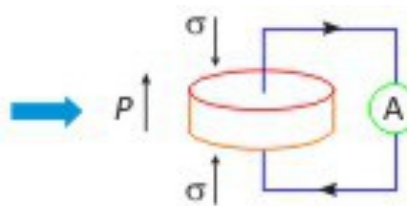


# Piezoelectric Effect

The **piezoelectric effect** is the ability of certain materials to generate an electric charge in response to applied mechanical stress, and conversely, to deform mechanically when an electric field is applied (converse effect).

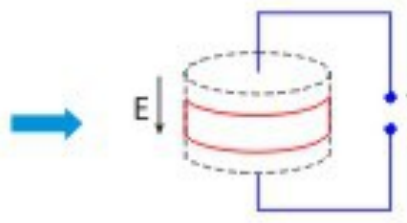
$$\mathbf{P} = \mathbf{e}\epsilon$$

Direct Piezoelectric Effect

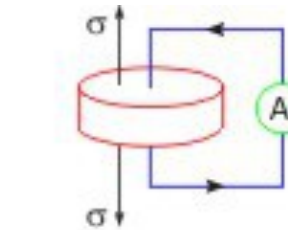


$$\epsilon = \mathbf{d}^T \mathbf{E}$$

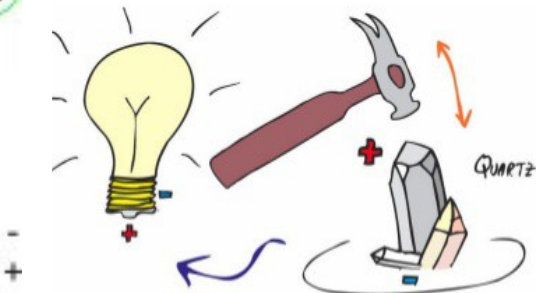
Converse Piezoelectric Effect



Contraction



Expansion



The piezoelectric effect (the name comes from piezein - Greek for “squeeze”) was discovered by the **Curie brothers** in 1880.

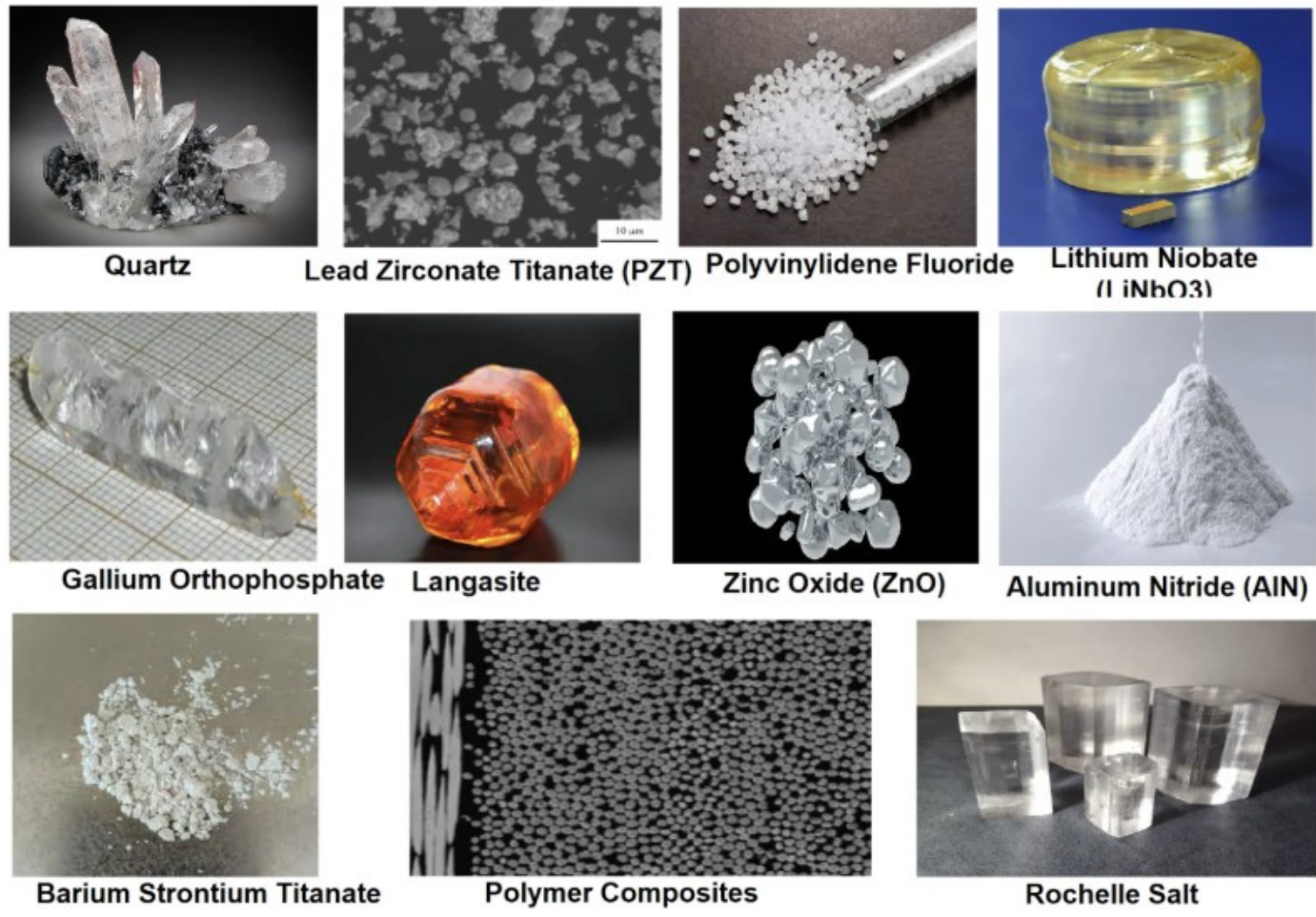
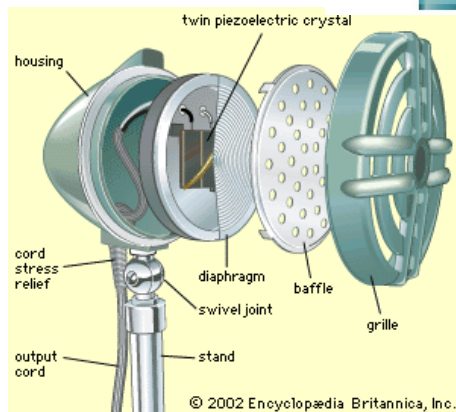
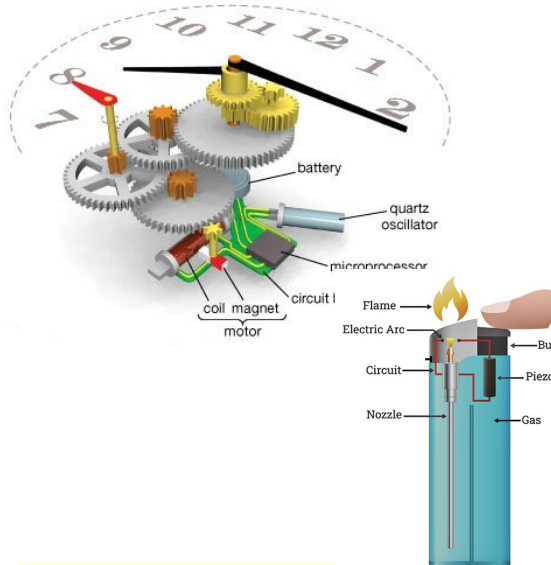


Jacques (left)  
and Pierre (right) Curie



# Piezoelectric Effect

Microphones, quartz watches, inkjet printers, lighters, all rely on an unusual phenomenon known as the piezoelectric effect found in various crystals, ceramics, and even bone and tendons.





# Piezoelectric Tensor

The **direct piezoelectric** effect is described by a **third-rank tensor e**:

$$P_i = \sum_v e_{iv} \epsilon_v \quad \text{so that} \quad e_{iv} = \left( \frac{\partial P_i}{\partial \epsilon_v} \right)_E$$

In CRYSTAL, direct piezoelectric constants can be computed:

- **Numerically**, from finite differences of the Berry phase computed at strained configurations;

$$e_{iv} = \frac{|e|}{2\pi V} \sum_l a_{li} \frac{\partial \varphi_l}{\partial \epsilon_v}$$

A. Erba, K. El-Kelany, M. Ferrero, I. Baraille, M. Rérat, Phys. Rev. B, 88, 035102 (2013)

- **Analytically**, from a Coupled-Perturbed Kohn-Sham approach.

$$\begin{aligned} \left. \frac{\partial}{\partial \varepsilon_i} \frac{\partial E^{TOT}}{\partial a_{\alpha j}} \right|_{\varepsilon=0, a^0} &= \text{Tr} \left( \left[ H^{(a_{\alpha j})} + \mathfrak{B}^{(a_{\alpha j})} + \frac{1}{2} \mathfrak{T}^{(a_{\alpha j})} \right] D^{(\varepsilon_i)} \right. \\ &\quad \left. + \left[ \frac{1}{2} \left( \mathfrak{q}^{(a_{\alpha j})} S + \mathfrak{T}^{(a_{\alpha j})} \right)^{(\varepsilon_i)} + \overline{M}_i^{(a_{\alpha j})} \right] D^{(0)} - S^{(a_{\alpha i})} D''_W^{(\varepsilon_i)} \right)_{a^0} \\ &\quad + \sum_A \zeta_A f_{A,\alpha} \delta_{ij} + e \delta_{ij} N_\alpha , , \end{aligned}$$

J. Baima, A. Erba, L. Maschio, C.M. Zicovich-Wilson, R. Dovesi and B. Kirtman  
Z. Phys. Chem., 230, 719-736 (2016)



# Piezoelectric Tensor

Also the piezoelectric effect can be formally decomposed into a purely **electronic** “**clamped-nuclei**” term due to the **instantaneous electronic response to strain**, and into a **nuclear-relaxation** term due to the rearrangement of atomic positions upon strain.

$$e_{iv} = \frac{\partial P_i}{\partial \epsilon_v} = e_{iv}^{\text{ele}} + e_{iv}^{\text{nuc}} \quad \text{where} \quad e_{iv}^{\text{ele}} = \left. \frac{\partial P_i}{\partial \epsilon_v} \right|_{\text{at. displ.}}$$

In CRYSTAL, the nuclear relaxation term can be computed following **two alternative approaches**:

- i) performing **geometry optimizations** to relax atomic positions at strained lattice configurations;
- ii) computing the **internal-strain tensor** of energy second-derivatives with respect to atomic displacements and lattice deformations, as combined with the **Born tensor**.

$$e_{iv}^{\text{nuc}} = -\frac{1}{V_0} \sum_{ai} Z_{k,ai}^* \Gamma_{ai,v} \quad \text{with} \quad Z_{k,ai}^* = \left. \frac{\partial^2 E}{\partial \epsilon_k \partial u_{ai}} \right|_{\eta}.$$

A. Erba, Phys. Chem. Chem. Phys., 18, 13984 (2016)

# Piezoelectric Tensor



The **direct piezoelectric** effect is described by a **third-rank tensor  $e$** , which, by resorting to **Voigt's notation**, can be given a  **$3 \times 6$  matrix representation**.

**Neumann's Principle** can be exploited to reduce the number of symmetry-independent components:

Triclinic

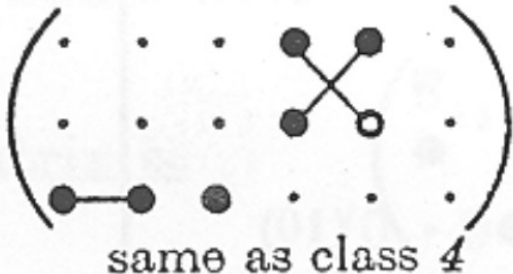
Class 1



(18)

Hexagonal

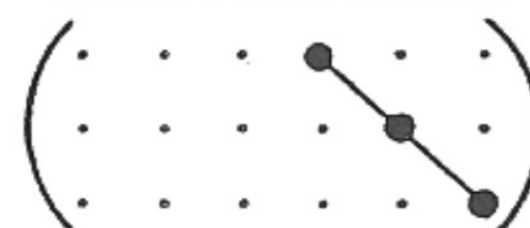
Class 6



(4)

Cubic

Classes  $\bar{4}3m$  and  $23$



(1)

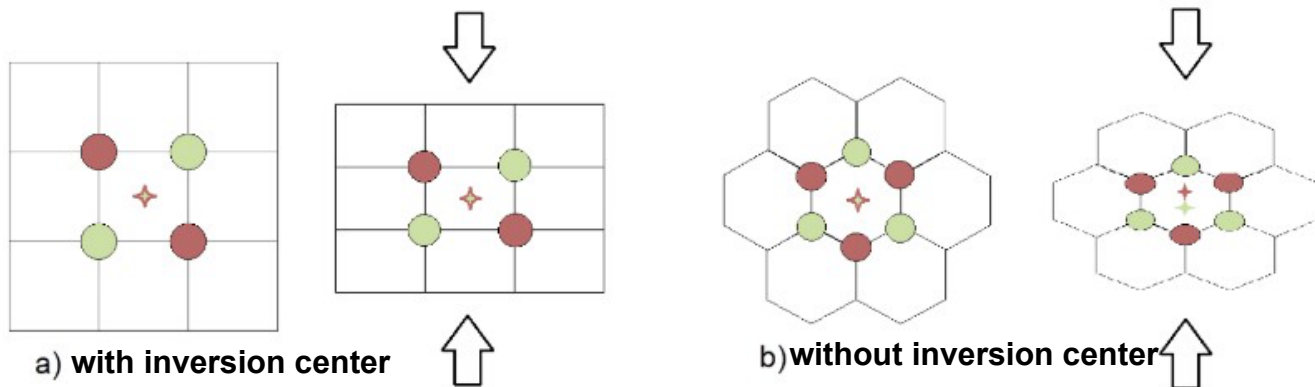
J. F. Nye, *Oxford University Press*, (1985)

Piezoelectricity has a very strong relation to the crystal symmetry that goes beyond Neumann's principle.



# Piezoelectric Tensor

**Piezoelectricity**, as well as **pyroelectricity** and **ferroelectricity**, is a material property that is strongly tied to crystal symmetries. Only crystals lacking an inversion symmetry are potentially piezoelectric.



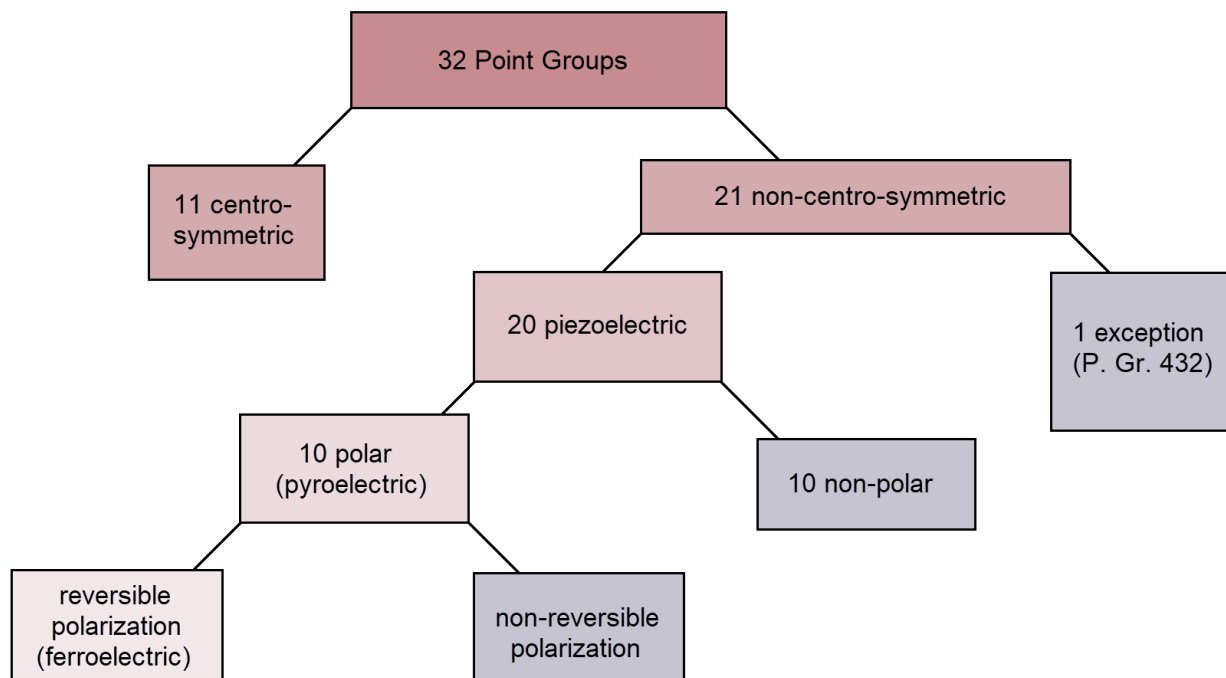
In Figure a), a plane of a cubic crystal like NaCl is shown. If no force is applied, the centers of charge of the positive and negative ions overlap and the overall polarization of this system is zero. If a force is applied, the atoms are pressed together horizontally, but the centers of charge still won't move due to the symmetry of the charged atoms at their respective corners; for an inversion-symmetric crystal, the polarization remains zero, even under stress.

In contrast, consider the hexagonal crystal without inversion symmetry in Figure b); this could represent a plane of Wurtzite ( $\beta$ -ZnS). The centers of charge of the positive and negative ions overlap again at the center of each cell without an external force, so the overall polarization in the crystal is zero. However, if a force is applied now, the centers of charge of the negative atoms and the positive atoms are suddenly shifted against each other due to their triangular symmetry. For each unit cell, a polarization appears, and thus the overall polarization of the non-inversion-symmetric crystal under stress is no longer zero.



# Piezoelectric Tensor

Of all 32 point groups, 21 are noncentrosymmetric, and of those 20 point groups show piezoelectricity (only point group 432 is an exception). Those piezoelectric point groups can be further divided into 10 polar and 10 nonpolar ones. The former exhibit spontaneous polarization and are called pyroelectric. For some of the pyroelectric groups, this spontaneous polarization can be reversed with an external electric field, and those materials are then called ferroelectrics.



11 centrosymmetric point groups: 1, 2/m, mmm, 4/m, 4/mmm, 3, 3m, 6/m, 6/mmm, m3, and m3m

21 noncentrosymmetric point groups:

exception: 432

20 piezoelectric:

10 polar: 1, 2, m, mm2, 3, 3m, 4, 4mm, 6, 6mm

10 nonpolar: 222, 4, 422, 42m, 32, 6, 622, 62m, 23, 43m



# Piezoelectric Tensor

The **converse piezoelectric effect** describes a strain induced by an electric field at constant stress and is described by a third-rank tensor  $\mathbf{d}$ :

$$\boldsymbol{\epsilon} = \mathbf{d}^T \mathbf{E}$$

It is linked to the direct piezoelectric tensor via the elastic tensor:

$$\mathbf{e} = \mathbf{d} \mathbb{C} \quad \text{and} \quad \mathbf{d} = \mathbf{e} \mathbb{S}$$

with

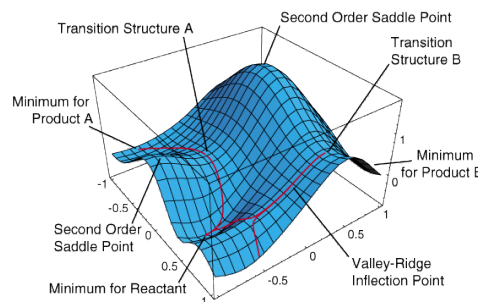
$$\mathbb{S} = \mathbb{C}^{-1}$$

In CRYSTAL, we compute it by combining the direct piezoelectric tensor with the elastic compliance tensor:

$$\mathbf{d} = \mathbf{e} \mathbb{S}$$



# Piezoelectric Tensor - Algorithm



Full structural relaxation

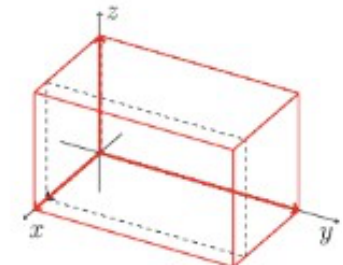


Berry phase calculation



Full symmetry analysis and definition  
of minimal set of strains

$$e_{iv} = \frac{\partial P_i}{\partial \epsilon_v} \Big|_0$$



$$\mathbf{e} = \mathbf{d} \mathbb{C} \quad \text{and} \quad \mathbf{d} = \mathbf{e} \mathbb{S}$$

Application of each strain, geometry optimization of atomic positions and calculation of cell gradients and Berry phase for different strain amplitudes



Piezoelectric constants are obtained by numerical fitting with respect to the strain



# Piezoelectric Tensor - Algorithm

In CRYSTAL, there is a fully-automated implementation that allows to compute the piezoelectric tensor of any material in a **single run**.

```
Geometry definition  
PIEZOC  
[Optional keywords]  
END  
END  
Basis set definition  
END  
Comput. Parameters  
END
```

A. Erba, K. El-Kelany, M. Ferrero, I. Baraille, M. Rérat, Phys. Rev. B, 88, 035102 (2013)



# Piezoelectric Tensor - Algorithm

In CRYSTAL, there is a fully-automated implementation that allows to compute the piezoelectric tensor of any material in a **single run**.

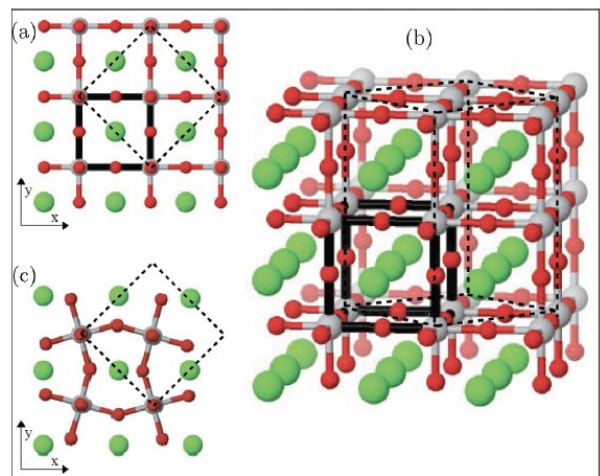
```
Geometry definition
ELAPIEZO
[Optional keywords]
END
END
Basis set definition
END
Comput. Parameters
END
```

A. Erba, K. El-Kelany, M. Ferrero, I. Baraille, M. Rérat, Phys. Rev. B, 88, 035102 (2013)



# Piezoelectric Tensor - Applications

## Piezoelectric response of SrTiO<sub>3</sub>



In 1997, Grupp and Goldman discovered a giant piezoelectric effect of strontium titanate (SrTiO<sub>3</sub>) down to 1.6 K, where the sole converse piezoelectric coefficient  $d_{31}$  was reported. The exact structure of SrTiO<sub>3</sub> at low temperature is unknown.

The anomalously large zero-point motion of Ti atoms, connected to the ferroelectric instability, is found to largely affect the piezoelectric response of SrTiO<sub>3</sub>.

A much stronger piezoelectric response is predicted to occur if the symmetry of the ferroelectric system is orthorhombic (as was recently theoretically suggested), rather than tetragonal.

TABLE V. Direct and converse piezoelectric constants of the two ferroelectric structures considered of SrTiO<sub>3</sub>. Electronic “clamped-ion” and total “relaxed,” with nuclear contribution, constants are reported. Calculations performed at the PBE0 level.

	Direct Piezoelectricity $\mathbf{e}$ (C/m <sup>2</sup> )							Converse Piezoelectricity $\mathbf{d}$ (pm/V)								
	$e_{11}$	$e_{31}$	$e_{12}$	$e_{13}$	$e_{33}$	$e_{24}$	$e_{35}$	$e_{26}$	$d_{11}$	$d_{31}$	$d_{12}$	$d_{13}$	$d_{33}$	$d_{24}$	$d_{35}$	$d_{26}$
<i>I4cm</i>																
Relaxed	0.20				8.82	4.86			-8.41				37.90	40.06		
Clamped	0.08				-0.13	0.05			0.29				-0.55	0.37		
<i>Ima2</i>																
Relaxed	9.28		6.70	0.20			4.61	6.04	33.51		20.08	-16.70		38.49	68.10	
Clamped	0.02		-0.06	0.06			0.04	-0.09	0.04		-0.26	0.24		0.31	-0.69	

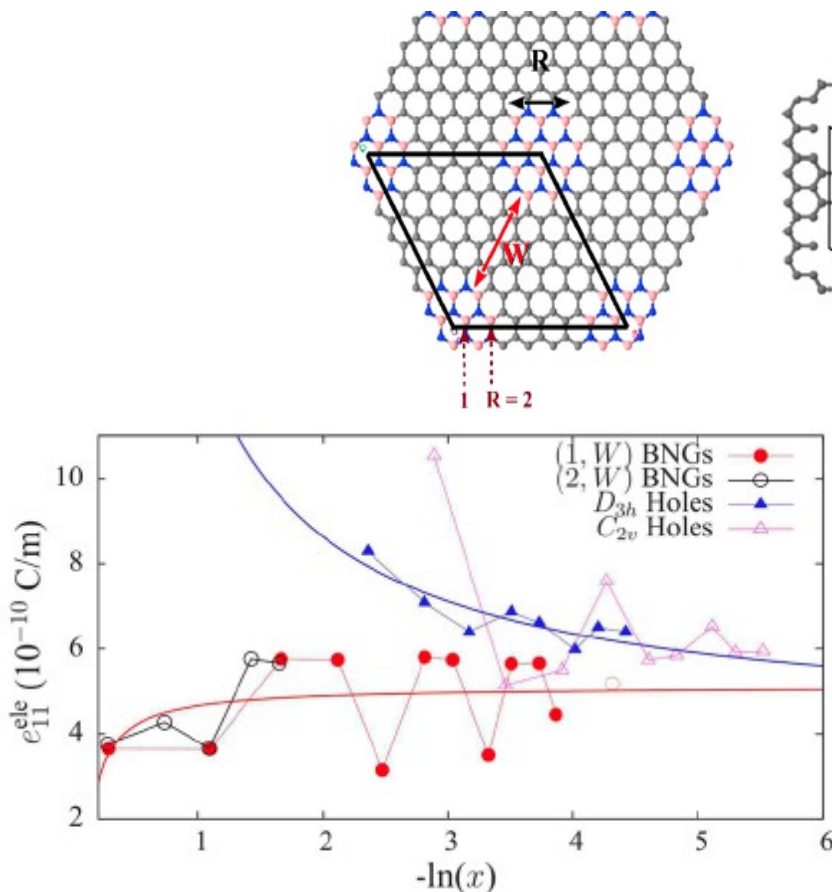


# Piezoelectric Tensor - Applications

We have also extended the calculation of piezoelectricity to 1D and 2D systems.

## Induced In-Plane Piezoelectricity in Graphene:

A finite in-plane piezoelectricity can be induced in graphene by breaking its inversion center with any in-plane defect, in the limit of vanishing defect concentration. We first considered different patterns of BN-doped graphene sheets and then other in-plane defects, such as holes of different symmetry.



The in-plane response is dominated by the electronic term and tends to a common limit value as the defect concentration decreases

Kh. E. El-Kelany, Ph. Carbonnière, A. Erba and M. Rérat, *J. Phys. Chem. C*, **119**, 8966-8973 (2015)



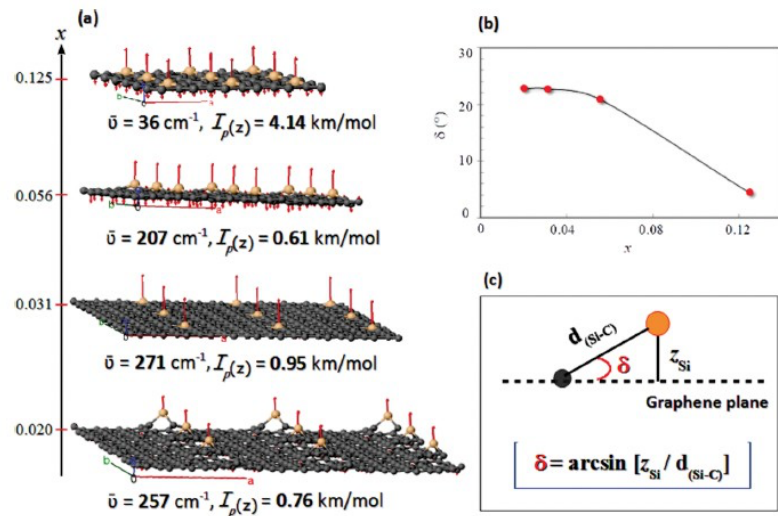
# Piezoelectric Tensor - Applications

We have also extended the calculation of piezoelectricity to 1D and 2D systems.

## Induced Out-of-Plane Piezoelectricity in Graphene:

A large out-of-plane piezoelectricity can be induced in graphene by carbon substitution. Several simple substitutions are considered where C atoms are replaced by heavier group-IV elements (Si, Ge, and Sn). A more complex functionalization (namely, pyrrolic N-doped graphene) is also investigated where different functional groups, such as F, Cl, H<sub>3</sub>C, and H<sub>2</sub>N, are studied.

The **combination** of an **out-of-plane symmetry-breaking defect** and a **soft IR-active phonon mode**, with a large cell-deformation coupling, is shown to constitute the necessary prerequisite to induce a large out-of-plane piezoelectric response into functionalized graphene.

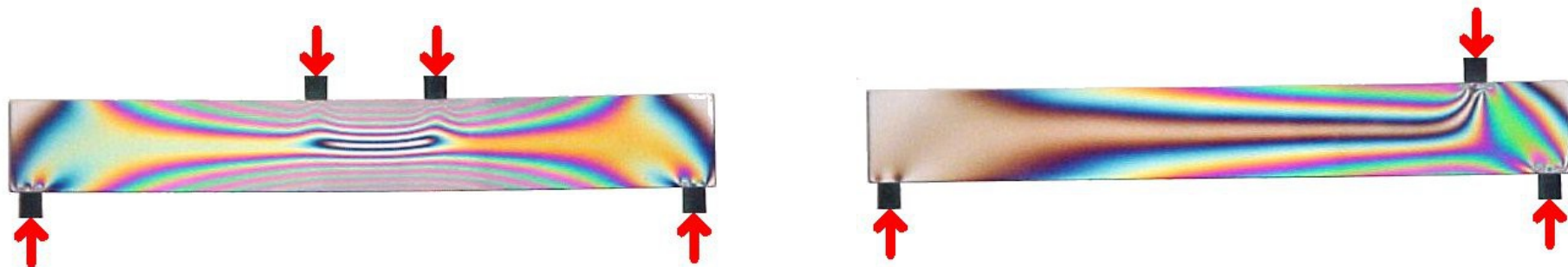


Kh. E. El-Kelany, Ph. Carbonnière, A. Erba, J.-M. Sotiroopoulos and M. Rérat, *J. Phys. Chem. C*, **120**, 7795-7803 (2016)

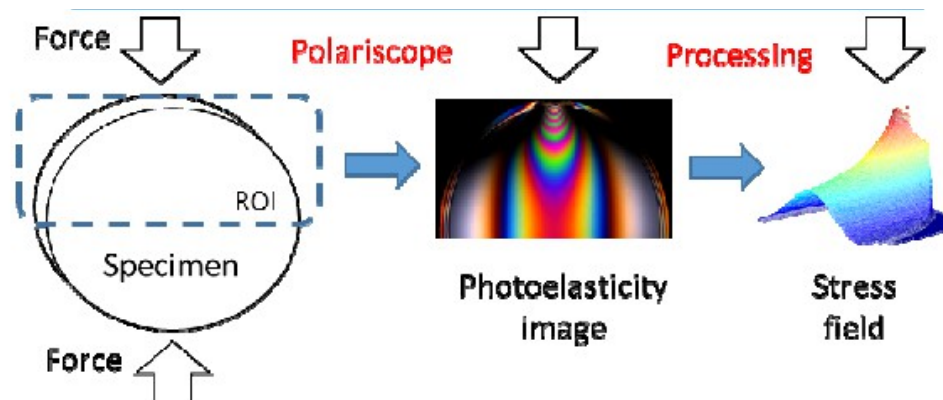


# Photoelastic Effect

In materials science, **photoelasticity** describes **changes in the optical properties of a material under mechanical deformation**. It is a property of all dielectric media and is often used to experimentally determine the stress distribution in a material.



Photoelasticity is an experimental method to determine the stress distribution in a material. The method is an important tool for determining critical stress points in a material, and is used for determining stress concentration in irregular geometries.





# Photoelastic Tensor

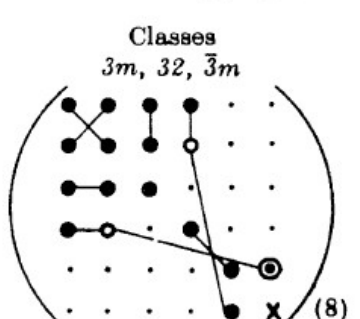
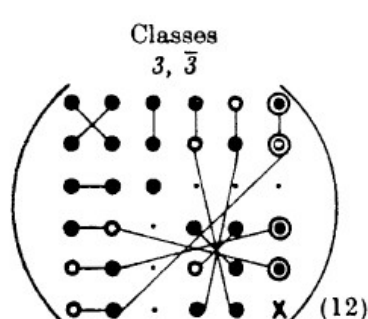
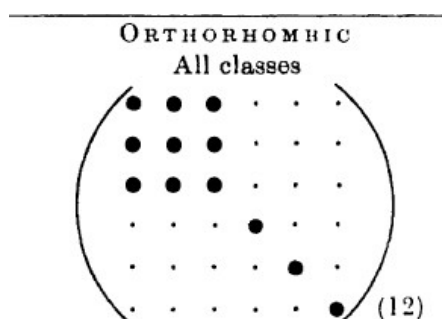
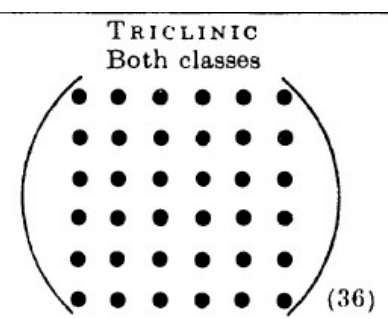
Formally, the **photoelastic** response of a material is described by a **fourth-rank tensor**:

$$p_{ijkl} = \frac{4\pi}{V} \frac{\partial^3 E}{\partial \epsilon_i \partial \epsilon_j \partial \eta_{kl}} = \frac{\partial \epsilon_{ij}}{\partial \eta_{kl}}$$

Both the **dielectric tensor  $\epsilon$**  and the **strain tensor  $\eta$**  are **symmetric**. Using Voigt's notation:

$$p_{vu} = \frac{\partial \epsilon_v}{\partial \eta_u} \quad \text{where} \quad p_{vu} \neq p_{uv}$$

So that the photoelastic tensor can be represented by a **6x6 matrix**:



J. F. Nye, *Oxford University Press*, (1985)



# Photoelastic Tensor - Implementation

In CRYSTAL, the photoelastic tensor is evaluated from numerical finite differences of the dielectric tensor computed at strained configurations. The dielectric tensor is computed via a CPHF/KS approach. **Single-run** algorithm.

Full structural relaxation and **Dielectric tensor** calculation through CPHF/KS



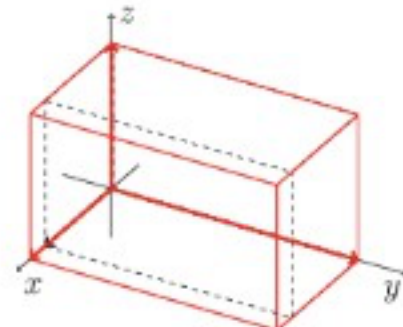
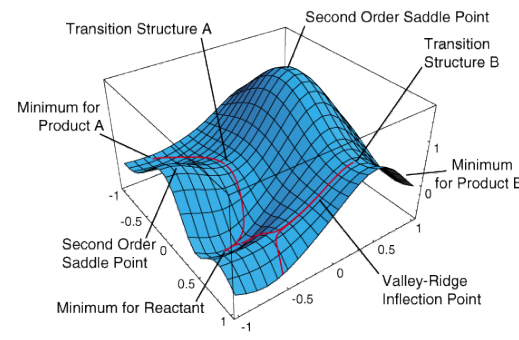
Full symmetry analysis and definition of minimal set of strains



Application of each strain, relaxation of atomic positions and calculation of cell gradients and the **dielectric tensor**



**Photoelastic constants** are obtained by numerical fitting with respect to the strain



A. Erba, R. Dovesi  
Phys. Rev. B, 88, 045121 (2013)



# Photoelastic Tensor - Implementation

In CRYSTAL, there is a fully-automated implementation that allows to compute the photoelastic tensor of any material in a **single run**.

```
Geometry definition
PHOTOELA
[Optional keywords]
END
END
Basis set definition
END
Comput. Parameters
END
```

A. Erba, R. Dovesi  
Phys. Rev. B, 88, 045121 (2013)



# Photoelastic Tensor - Implementation

As a validation of the implementation, we have computed the photoelastic properties of several simple crystals for which accurate experimental data exist:  
**MgO, NaCl, LiF, KCl, Silicon, Diamond, Quartz, Rutile.**

	HF	LDA	PBE	PBE0	EXP.	Diamond	$\epsilon^{el}$	4.974	5.668	5.749	5.443	5.819 <sup>69</sup>
NaCl						$p_{11}$	-0.302	-0.264	-0.270	(-0.270)	-0.268	-0.248 <sup>70</sup>
$\epsilon^{el}$	1.395	2.615	2.430		2.330	$p_{12}$	0.056	0.076	0.073	(0.073)	0.072	0.044 <sup>70</sup>
$p_{11}$	0.308	0.077	0.119	(0.119)	0.136	$p_{44}$	-0.214	-0.162	-0.175	(-0.189)	-0.175	-0.172 <sup>70</sup>
$p_{12}$	0.194	0.157	0.166	(0.166)	0.185	$\alpha$ -Quartz						
$p_{44}$	-0.022	-0.002	-0.007	(-0.007)	-0.005	$\epsilon_{xx}^{el}$	1.935	2.453	2.347		2.209	2.356 <sup>26</sup>
LiF						$\epsilon_{zz}^{el}$	1.950	2.497	2.384		2.238	2.383 <sup>26</sup>
$\epsilon^{el}$	1.448	2.042	1.975		1.894	$p_{11}$	0.168	0.203	0.160	(-0.202)	0.173	0.160 <sup>23</sup>
$p_{11}$	0.231	-0.044	-0.026	(-0.026)	0.000	$p_{12}$	0.304	0.289	0.297	(0.073)	0.304	0.270 <sup>23</sup>
$p_{12}$	0.219	0.139	0.136	(0.136)	0.155	$p_{13}$	0.313	0.299	0.298	(0.029)	0.312	0.270 <sup>23</sup>
$p_{44}$	-0.045	-0.051	-0.054	(-0.054)	-0.055	$p_{33}$	0.148	0.112	0.107	(-0.197)	0.126	0.100 <sup>23</sup>
MgO						$p_{14}$	-0.047	-0.052	-0.059	(-0.010)	-0.055	-0.047 <sup>23</sup>
$\epsilon^{el}$	1.848	3.077	3.097		2.868	$p_{44}$	-0.066	-0.075	-0.089	(-0.166)	-0.081	-0.079 <sup>23</sup>
$p_{11}$	-0.127	-0.218	-0.213	(-0.213)	-0.195	$\epsilon_{xx}^{el}$	3.404	7.476	7.266		5.478	6.840 <sup>16</sup>
$p_{12}$	0.091	0.013	0.015	(0.015)	0.037	$\epsilon_{zz}^{el}$	3.934	9.054	9.027		6.684	8.430 <sup>16</sup>
$p_{44}$	-0.147	-0.075	-0.078	(-0.078)	-0.083	$p_{11}$	0.008	0.020	0.038	(-0.042)	0.033	0.012 <sup>16</sup>
KCl						$p_{12}$	0.235	0.137	0.166	(0.104)	0.204	0.144 <sup>16</sup>
$\epsilon^{el}$	1.908	2.396	2.199		2.125	$p_{13}$	-0.011	-0.094	-0.130	(-0.195)	-0.107	-0.140 <sup>16</sup>
$p_{11}$	0.289	0.230	0.257	(0.257)	0.272	$p_{33}$	-0.040	-0.040	-0.075	(-0.058)	-0.068	-0.057 <sup>16</sup>
$p_{12}$	0.202	0.175	0.181	(0.181)	0.192	$p_{44}$	-0.023	-0.004	0.000	(0.039)	-0.010	x
$p_{44}$	-0.044	-0.035	-0.046	(-0.046)	-0.044	$p_{66}$	-0.067	-0.064	-0.082	(-0.082)	-0.087	-0.062 <sup>16</sup>
Silicon						$ \Delta p $	18.0	4.1	1.9	(3.2)	6.2	-
$\epsilon^{el}$	7.952	10.468	12.087		10.409	<td></td> <td></td> <td></td> <td></td> <td></td> <td></td>						
$p_{11}$	-0.163	-0.111	-0.107	(-0.107)	-0.109	<td></td> <td></td> <td></td> <td></td> <td></td> <td></td>						
$p_{12}$	0.000	0.020	0.010	(0.010)	0.021	<td></td> <td></td> <td></td> <td></td> <td></td> <td></td>						
$p_{44}$	-0.100	-0.056	-0.054	(-0.093)	-0.055	<td></td> <td></td> <td></td> <td></td> <td></td> <td></td>						

A. Erba, R. Dovesi, Phys. Rev. B, 88, 045121 (2013)



# Photoelastic Tensor - Implementation

As a validation of the implementation, we have computed the photoelastic properties of several simple crystals for which accurate experimental data exist: **MgO, NaCl, LiF, KCl, Silicon, Diamond, Quartz, Rutile.**

TABLE IV: Elasto-optic constants of the MgO crystal as experimentally measured by various workers, compared with the results of the present study.

	$p_{11} - p_{12}$	$p_{44}$	$p_{11}$	$p_{12}$
Giardini <i>et al.</i> <sup>68</sup>	-0.25	-0.10	-0.21	+0.04
Vedam <i>et al.</i> <sup>10</sup>	-0.248	×	-0.259	-0.011
Burstein <i>et al.</i> <sup>71</sup>	-0.24	×	-0.3	-0.08
Krishna Rao <i>et al.</i> <sup>72</sup>	-0.24	-0.105	-0.31	-0.07
West <i>et al.</i> <sup>73</sup>	-0.253	-0.096	×	×
Present work LDA	-0.231	-0.075	-0.218	+0.013
Present work PBE	-0.228	-0.078	-0.213	+0.015

MgO



# Photoelastic Tensor - Implementation

As a validation of the implementation, we have computed the photoelastic properties of several simple crystals for which accurate experimental data exist: **MgO, NaCL, LiF, KCl, Silicon, Diamond, Quartz, Rutile.**

TABLE IV: Elasto-optic constants of the MgO crystal as experimentally measured by various workers, compared with the results of the present study.

	$p_{11} - p_{12}$	$p_{44}$	$p_{11}$	$p_{12}$
Giardini <i>et al.</i> <sup>68</sup>	-0.25	-0.10	-0.21	+0.04
Vedam <i>et al.</i> <sup>10</sup>	-0.248	×	-0.259	-0.011
Burstein <i>et al.</i> <sup>71</sup>	-0.24	×	-0.3	-0.08
Krishna Rao <i>et al.</i> <sup>72</sup>	-0.24		-0.105	-0.31
West <i>et al.</i> <sup>73</sup>	-0.253	-0.096	×	×
Present work LDA	-0.231	-0.075	-0.218	+0.013
Present work PBE	-0.228	-0.078	-0.213	+0.015

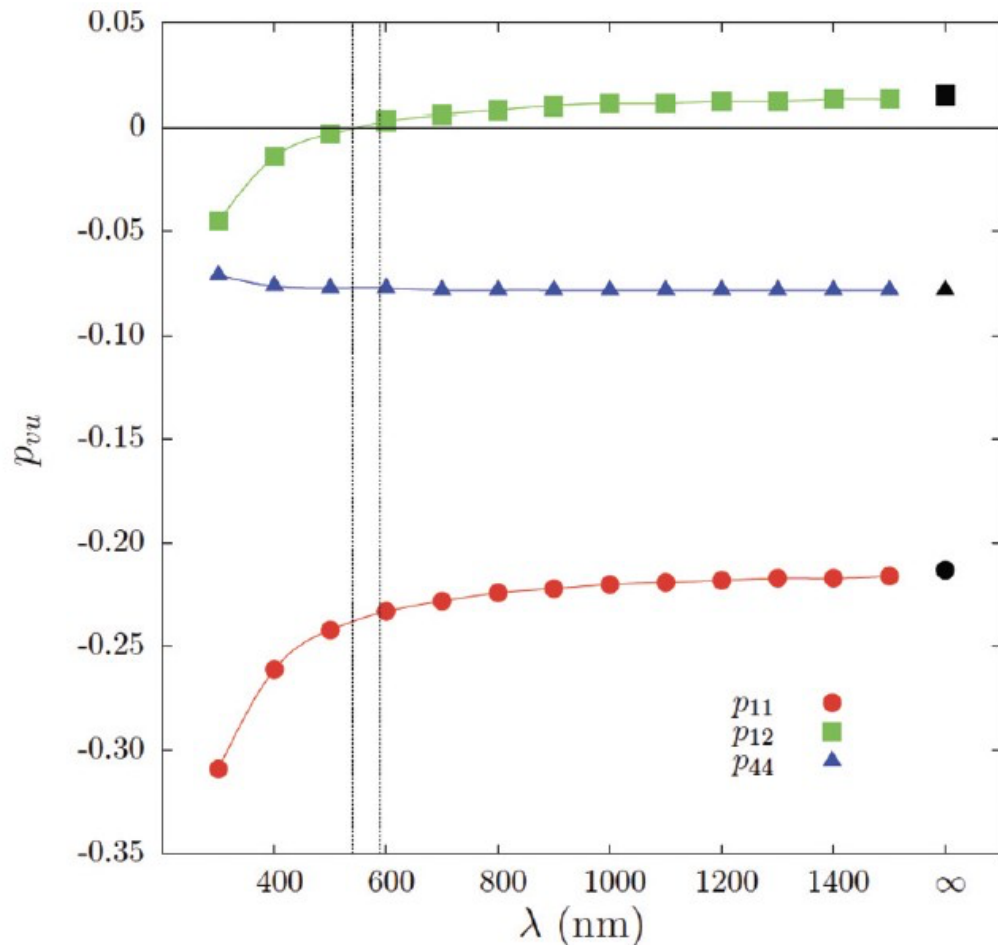
MgO



# Photoelastic Tensor - Implementation

As a validation of the implementation, we have computed the photoelastic properties of several simple crystals for which accurate experimental data exist:  
**MgO, NaCL, LiF, KCl, Silicon, Diamond, Quartz, Rutile.**

MgO



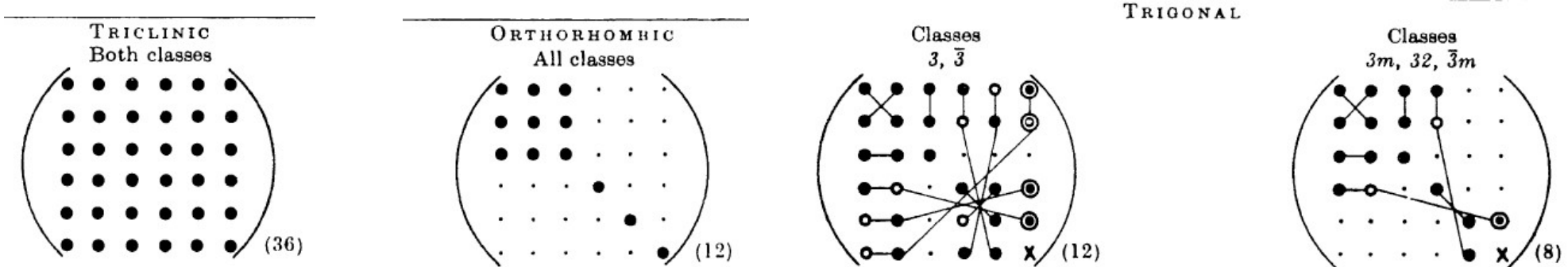


# Piezo-Optic Tensor

The **piezo-optic tensor  $\pi$**  can be computed by combining the photo-elastic tensor with the elastic compliance tensor:

$$\pi = \mathbf{p} \mathbb{S} \quad \text{and conversely} \quad \mathbf{p} = \pi \mathbb{C}$$

It is also a **fourth-rank** tensor:



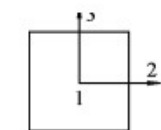
In CRYSTAL, we have a fully-automated implementation for the single-run calculation of the piezo-optic tensor.

A. Erba, M.T. Ruggiero, T. M. Korter and R. Dovesi, J. Chem. Phys., 143, 144504 (2015).

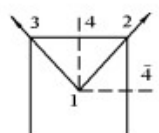


# Piezo-Optic Tensor - Experiments

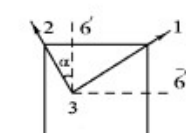
The experimental piezo-optical characterization of a crystal is very **challenging**. For instance, 57 measurements on 16 differently cut samples are necessary (with specific orientations of the laser with the sample) to determine the 36 independent piezo-optic constants of a triclinic system



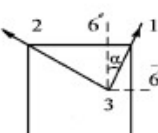
Sample No.1



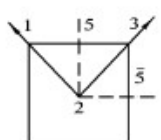
Sample No.2



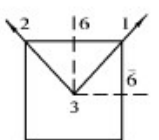
Sample No.9



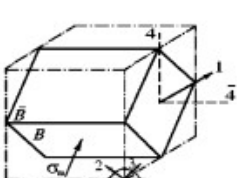
Sample No.10



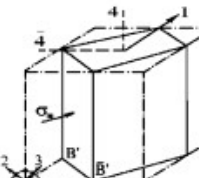
Sample No.3



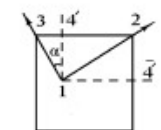
Sample No.4



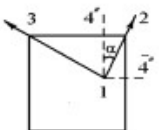
Sample No.11



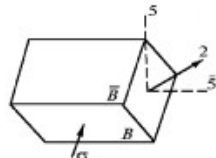
Sample No.12



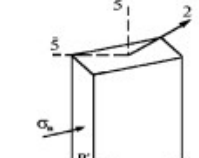
Sample No.5



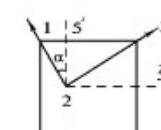
Sample No.6



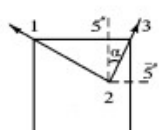
Sample No.13



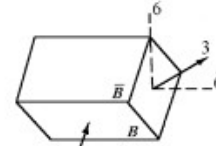
Sample No.14



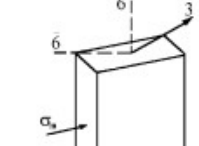
Sample No.7



Sample No.8



Sample No.15



Sample No.16



# Piezo-Optic Tensor - Experiments

The experimental piezo-optical characterization of a crystal is very **challenging**. For instance, 57 measurements on 16 differently cut samples are necessary (with specific orientations of the laser with the sample) to determine the 36 independent piezo-optic constants of a triclinic system

Table 2

Supplement to Table 1: Additional relationship for the calculation of piezooptic constants for the crystals of higher symmetries

No.	Crystal system (class of symmetry)	Necessary samples	Number of measur.	No. of equation	Additional relationships and cases of their application
1	Monoclinic (all classes)	8 samples: no. 1; 2; 3; 4; 7; 8; 11; 15	29	T.29	$\pi_{46} = 2\sqrt{2}n_4^{-3}\left(\frac{\delta\Delta_{4\bar{1}\bar{6}}}{t_4\sigma_B} - \frac{\delta\Delta_{4\bar{4}\bar{6}}}{t_4\sigma_B}\right) + n_4^{-3}(n_4 - 1)(S_{25} + S_{35} - S_{46}) - (\pi_{25} + \pi_{35})/2$ (sample no. 12 is not needed)
				T. 30	$\pi_{64} = 2\sqrt{2}n_6^{-3}\left(\frac{\delta\Delta_{6\bar{6}\bar{8}}}{t_6\sigma_B} - \frac{\delta\Delta_{6\bar{6}\bar{8}}}{t_6\sigma_B}\right) + n_6^{-3}(n_6 - 1)(S_{15} + S_{25} - S_{46}) - (\pi_{15} + \pi_{25})/2$ (sample no. 16 is not needed) $\pi_{44}, \pi_{66}$ —according to (T.31)
2	Orthorombic (all classes)	4 samples: no. 1; 2; 3; 4	12	T.31	$\pi_{rr} = -4n_r^{-3}\frac{\delta\Delta_{\bar{r}\bar{i}\bar{r}}}{t_r\sigma_r} + n_r^{-3}(n_r - 1)(S_{ii} + S_{jj} + 2S_{ij} - S_{rr}) - (\pi_{ii} + \pi_{jj} + \pi_{ii} + \pi_{jj})/2$ , where $r = 9 - i - j$ and $i \neq j = 1, 2$ or 3 (only one measurement on samples no. 2, 3 and 4 for determination of $\pi_{44}, \pi_{55}$ and $\pi_{66}$ , respectively)
3	Trigonal (3, $\bar{3}$ )	5 samples: no. 1; 2; 3; 4; 11	19	T.32	$\pi_{45} = 2\sqrt{2}n_4^{-3}\left(\frac{\delta\Delta_{4\bar{1}\bar{6}}}{t_4\sigma_B} - \frac{\delta\Delta_{4\bar{4}\bar{6}}}{t_4\sigma_B}\right) + n_4^{-3}(n_4 - 1)(S_{25} - S_{16} - S_{45}) - (\pi_{25} - \pi_{16} + 4\pi_{52})/2$ -(sample no. 12 is not needed)
4	Trigonal (32, 3 m, $\bar{3}$ m)	2 samples: no. 1; 2	11		No difference
5	Tetragonal (4, $\bar{4}$ , 4/m)	6 samples: no. 1; 2; 4; 9; 10; 11	14	T.33	$\pi_{61} = \frac{4\sqrt{3}}{3}n_{6'}^{-3}\left(\frac{\delta\Delta_{\bar{6}'\bar{6}'}}{t_{6'}\sigma_{6'}} - \frac{\delta\Delta_{\bar{6}'\bar{6}'}}{t_{6''}\sigma_{6''}}\right) - 2n_{6'}^{-3}(n_6 - 1)S_{16} - \pi_{16}/2$ -more suitable, because $\pi_{62} = -\pi_{61}$ $\pi_{45}$ —according to (T.32), but if takes into account that: $\pi_{25} = \pi_{52} = 0$ and $S_{25} = S_{45} = 0$ ; $\pi_{44}$ —according to (T.31)
6	Tetragonal (422, 4 mm, 4/mmm)	3 samples: no. 1; 2; 4	7		$\pi_{44}, \pi_{66}$ —according to T.31
7	Hexagonal (6, $\bar{6}$ , 6/m)	4 samples: no. 1; 2; 4; 11	10		$\pi_{45}, \pi_{44}$ -analogously to sample no. 5 of tetragonal system
8	Hexagonal (622, 6/mmm, 6 mm, $\bar{6}m2$ )	2 samples: no. 1; 2	6		$\pi_{44}$ —according to (T.31)
9	Cubic (23, m3)	2 samples: no. 1; 2	4		$\pi_{44}$ —according to (T.31)
10	Cubic (432, 43 m, m3m)	2 samples: no. 1; 2	3		$\pi_{44}$ —according to (T.31)



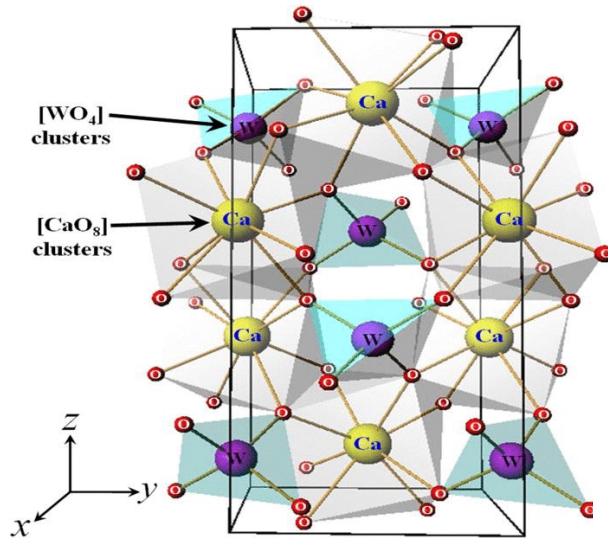
# Piezo-Optic Tensor - Experiments

The experimental piezo-optical characterization of a crystal is very **challenging**. For instance, 57 measurements on 16 differently cut samples are necessary (with specific orientations of the laser with the sample) to determine the 36 independent piezo-optic constants of a triclinic system



Bohdan Mytsyk  
Lviv, Ukraine

# Piezo-Optic Tensor – Applications – CaWO<sub>4</sub>

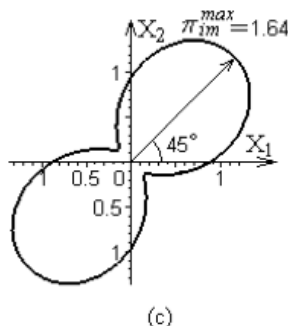
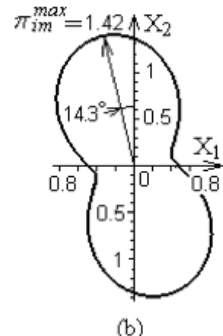
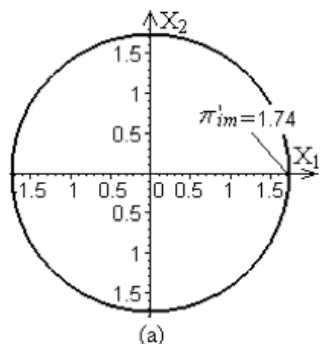
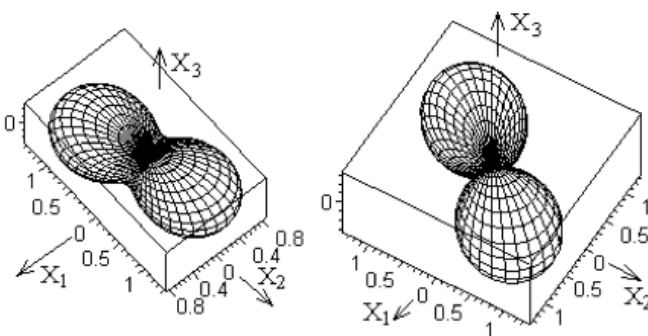
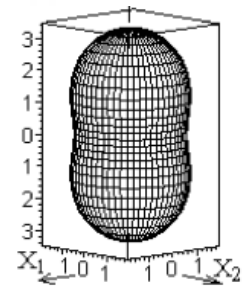
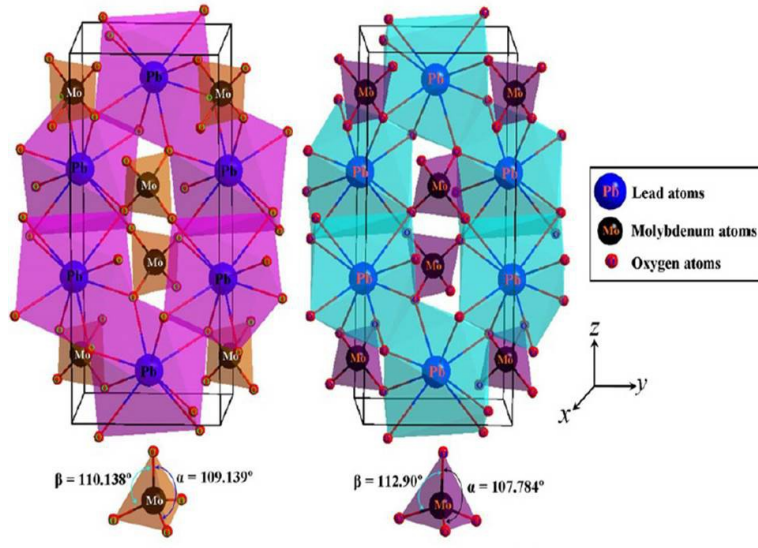


A. Erba, M.T. Ruggiero, T. M. Korter and R. Dovesi,  
J. Chem. Phys., 143, 144504 (2015).

	Photoelastic constants									
	<i>P</i> <sub>11</sub>	<i>P</i> <sub>12</sub>	<i>P</i> <sub>13</sub>	<i>P</i> <sub>31</sub>	<i>P</i> <sub>33</sub>	<i>P</i> <sub>44</sub>	<i>P</i> <sub>45</sub>	<i>P</i> <sub>16</sub>	<i>P</i> <sub>61</sub>	<i>P</i> <sub>66</sub>
SVWN	0.154	0.150	0.263	0.254	0.201	0.018	-0.018	0.051	0.029	-0.071
PBE	0.157	0.175	0.249	0.256	0.226	0.018	-0.017	0.022	0.026	-0.058
B3LYP	0.152	0.194	0.240	0.264	0.208	0.009	-0.017	0.019	0.026	-0.050
PBE0	0.177	0.185	0.255	0.265	0.229	0.014	-0.019	0.032	0.025	-0.055
Expt.	0.40	-0.02	0.24	0.25	0.21	0.011	-0.06	-0.27	0.025	-0.031
									(-0.001)	(-0.018)
	Piezo-optic constants (Br ≡ TPa <sup>-1</sup> )									
	$\pi_{11}$	$\pi_{12}$	$\pi_{13}$	$\pi_{31}$	$\pi_{33}$	$\pi_{44}$	$\pi_{45}$	$\pi_{16}$	$\pi_{61}$	$\pi_{66}$
SVWN	0.417	-0.035	1.467	0.788	0.578	0.352	-0.345	1.006	0.058	-1.151
PBE	0.308	0.387	1.706	0.946	1.001	0.436	-0.404	0.430	0.128	-1.104
B3LYP	0.256	0.622	1.480	1.030	0.759	0.202	-0.384	0.283	0.149	-0.896
PBE0	0.495	0.367	1.508	0.938	0.922	0.318	-0.409	0.637	0.100	-0.964
Expt.	1.86	-0.60	1.52	1.02	1.01	0.33	-1.77	-5.64	0.16	-0.63



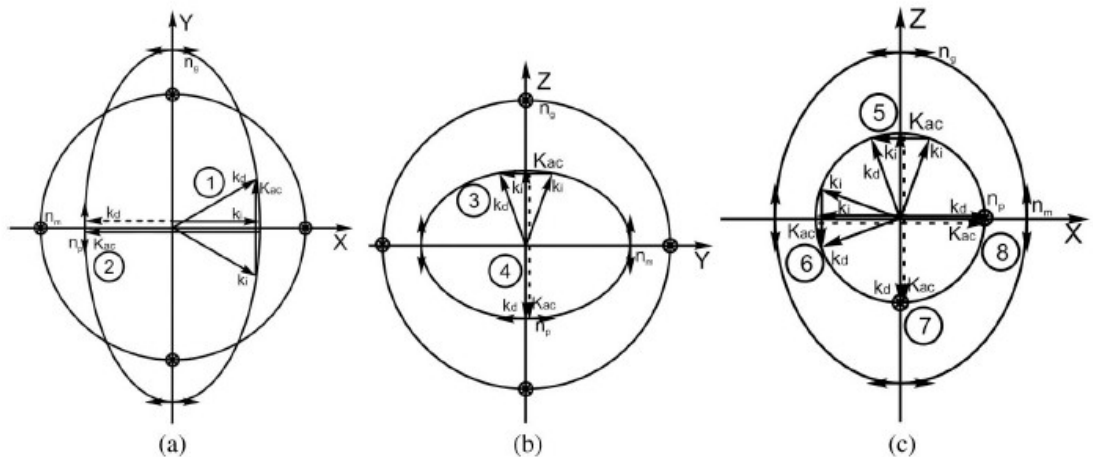
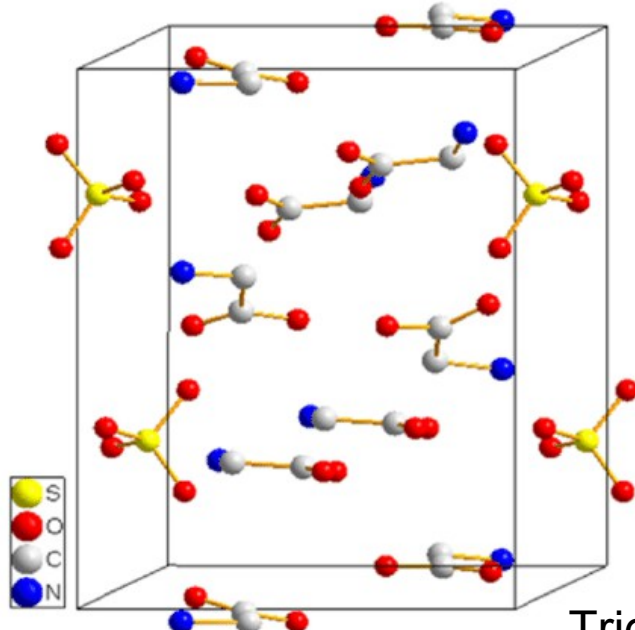
# Piezo-Optic Tensor – Applications – PbMoO<sub>4</sub>



B. Mytsyk, A. Erba, N. Demyanyshyn and A. Saharuk  
Opt. Mater. 62, 632-638 (2016)

$\pi_{im}$	$\pi_{11}$	$\pi_{12}$	$\pi_{13}$	$\pi_{31}$	$\pi_{33}$	$\pi_{44}$	$\pi_{45}$	$\pi_{16}$	$\pi_{61}$	$\pi_{66}$
This work	0.480	1.361	1.737	0.036	3.340	1.806	0.184	-0.895	-0.241	1.509
$p_{in}$	$p_{11}$	$p_{12}$	$p_{13}$	$p_{31}$	$p_{33}$	$p_{44}$	$p_{45}$	$p_{16}$	$p_{61}$	$p_{66}$
This work	0.247	0.263	0.258	0.178	0.318	0.049	0.005	-0.023	-0.030	0.064
[2]	0.24	0.24	0.255	0.175	0.300	0.067	-0.01	0.017	0.013	0.05
[4]	0.28	0.28	0.35	0.14	0.28	—	—	-0.01	0.05	0.04

# Piezo-Optic Tensor – Applications – TGS



Triglycine sulfate crystal

$p_{11}$	$p_{22}$	$p_{33}$	$p_{12}$	$p_{21}$	$p_{13}$	$p_{31}$	$p_{23}$	$p_{32}$	$p_{44}$
0.128 ±0.064	0.288 ±0.039	$0.183 \pm 0.039$	0.125 ±0.083	0.227 ±0.055	0.196 ±0.080	0.139 ±0.031	0.256 ±0.043	0.149 ±0.032	-0.035 ±0.021
$p_{55}$	$*p_{66}$	$*p_{46}$	$p_{64}$	$*p_{51}$	$p_{52}$	$p_{53}$	$p_{15}$	$p_{25}$	$p_{35}$
0.054 ±0.026	0.012 ±0.014	0.005 ±0.013	0.161 ±0.030	0.042 ±0.075	0.146 ±0.034	0.097 ±0.036	-0.102 ±0.024	-0.043 ±0.009	-0.058 ±0.020

B. Mytsyk, N. Demyanyshyn, A. Erba, V. Shut, S. Mozzharov, Y. Kost, O. Mys and R. Vlokh,  
Appl. Opt., 56 9484-9490 (2017)

# Piezo-Optic Tensor – Applications – CNGS



$\text{Ca}_3\text{TaGa}_3\text{Si}_2\text{O}_{14}$  (CTGS) and  $\text{Ca}_3\text{NbGa}_3\text{Si}_2\text{O}_{14}$  (CNGS)

B. Mytsyk, A. Erba, J. Maul, N. Demyanyshyn,  
P. Shchepanskyi, and O. Syrotynskyi  
Appl. Opt., 62, 7952-7959 (2023)

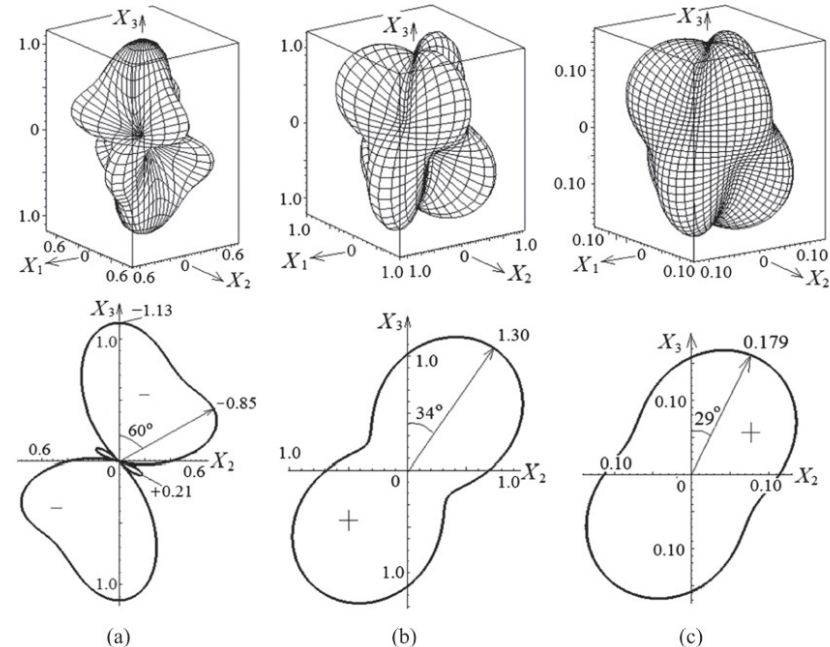
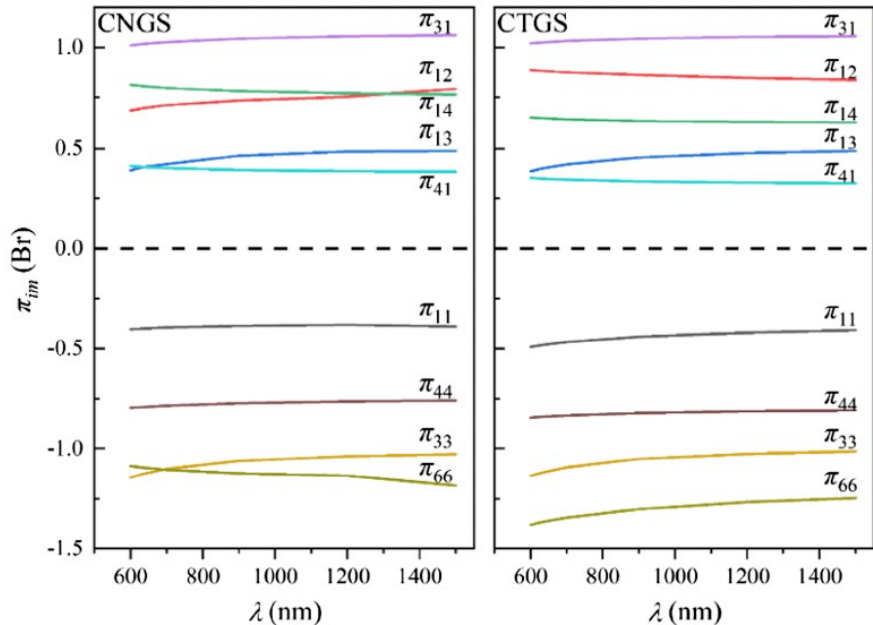
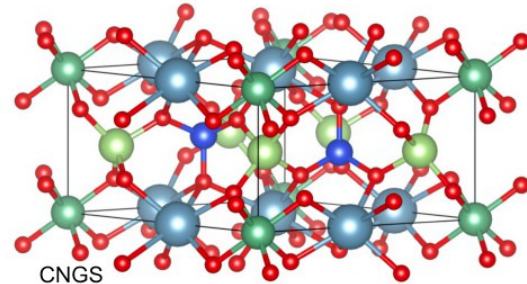


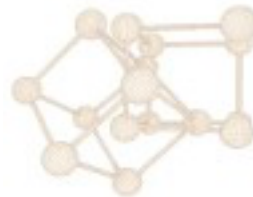
Table 1. All Independent Piezo-Optic Coefficients  $\pi_{im}$  of CNGS and CTGS Crystals<sup>a</sup>

$\pi_{im}$	$\pi_{11}$	$\pi_{12}$	$\pi_{13}$	$\pi_{31}$	$\pi_{33}$	$\pi_{14}$	$\pi_{41}$	$\pi_{44}$
CNGS (calculation)	-0.40	0.69	0.41	1.02	-1.13	0.81	0.41	-0.79
CTGS (calculation)	-0.48	0.88	0.40	1.03	-1.12	0.65	0.35	-0.84
CTGS (experiment [33])	$-0.19 \pm 0.06$	$0.22 \pm 0.09$	$0.53 \pm 0.12$	$1.40 \pm 0.19$	$-1.20 \pm 0.09$	$0.72 \pm 0.11$	$0.32 \pm 0.11$	$-0.81 \pm 0.40$

<sup>a</sup>in units of Br, 1 Br = 1 Brewster =  $10^{-12} \text{ m}^2/\text{N}$ .

Table 2. All Independent Elasto-Optic Coefficients  $p_{ik}$  of CNGS and CTGS Crystals

$p_{ik}$	$p_{11}$	$p_{12}$	$p_{13}$	$p_{31}$	$p_{33}$	$p_{14}$	$p_{41}$	$p_{44}$
CNGS (calculation)	0.017	0.116	0.119	0.160	-0.107	0.036	0.037	-0.036
CTGS (calculation)	0.019	0.137	0.126	0.163	-0.104	0.031	0.031	-0.039
CTGS (experiment [33])	$0.008 \pm 0.010$	$0.044 \pm 0.013$	$0.096 \pm 0.022$	$0.165 \pm 0.031$	$-0.088 \pm 0.031$	$0.029 \pm 0.031$	$0.029 \pm 0.015$	$-0.033 \pm 0.017$



Advanced School on  
**QUANTUM MODELLING**  
of Materials with CRYSTAL

Thank You for your Attention